

ESPRESSO: Robust Concept Filtering in Text-to-Image Models

Anudeep Das
University of Waterloo
anudeep.das@uwaterloo.ca

Rui Zhang
Zhejiang University
zhangrui98@zju.edu.cn

Vasisht Duddu
University of Waterloo
vasisht.duddu@uwaterloo.ca

N. Asokan
University of Waterloo
asokan@acm.org

ABSTRACT

Diffusion based text-to-image (T2I) models generate high fidelity images for given textual prompts. They are trained on large datasets scraped from the Internet, potentially containing *unacceptable concepts* (e.g., copyright infringing or unsafe). Retraining T2I models after filtering out unacceptable concepts in the training data is inefficient and degrades utility. Hence, there is a need for concept removal techniques (CRTs) which are i) *effective* in removing unacceptable concepts, ii) *utility-preserving* on acceptable concepts, and, iii) *robust* against evasion with adversarial prompts. None of the prior CRTs satisfy all these requirements simultaneously.

We introduce ESPRESSO, the first *robust concept filter* based on Contrastive Language-Image Pre-Training (CLIP). It identifies unacceptable concepts by projecting the generated image’s embedding onto the vector connecting both unacceptable and acceptable concepts in the joint text-image embedding space. This ensures robustness by restricting the adversary to adding noise *only* along this vector, in the direction of the acceptable concept. Further fine-tuning ESPRESSO to separate embeddings of acceptable and unacceptable concepts, while preserving their pairing with image embeddings, ensures both effectiveness and utility. We evaluate ESPRESSO on eleven concepts to show that it is effective (~5% CLIP accuracy on unacceptable concepts), utility-preserving (~93% normalized CLIP score on acceptable concepts), and robust (~4% CLIP accuracy on adversarial prompts for unacceptable concepts). Finally, we present theoretical bounds for certified robustness of ESPRESSO against adversarial prompts, and an empirical analysis.

1 INTRODUCTION

Diffusion based text-to-image (T2I) models have demonstrated a remarkable ability to generate high quality images from textual prompts [44, 46, 47]. These models are trained on large datasets of unfiltered content from the Internet [43, 50]. Due to their large capacity, T2I models memorize specific *concepts*, as seen in the generated images [4, 25, 52]. Some of these concepts, may be *unacceptable* for various reasons such as copyright infringement (e.g., a movie character or celebrity) or inappropriateness (e.g., “nudity” or “violence”) [13, 18, 49]. Retraining T2I models after filtering out unacceptable concepts is inefficient, only partially effective [30, 48], and compromises utility [13]. Hence, there is a need for *concept removal techniques* (CRTs) to minimize unacceptable concepts in generated images.

Ideally, CRTs should be *effective* in reducing the generation of unacceptable concepts while preserving the *utility* on all others, and *robust* to evasion with adversarial prompts. As we show in Section 6, none of the existing CRTs *simultaneously* satisfy these

requirements: i) *filtering* CRTs, which detect unacceptable concepts, lack robustness ([45] and Section 6.2), ii) *fine-tuning* CRTs which modify T2I models, trade-off effectiveness and utility [13, 18, 27, 49], and lack robustness [38, 53, 57, 63]. Designing a CRT meeting all the requirements is an open problem. Our goal is to design such a CRT.

We opt to use a filter as it will not alter the T2I model, thus reducing its impact on utility. We construct our filter using the Contrastive Language-Image Pre-Training (CLIP) [43], an essential component of T2I models. CLIP co-locates the embeddings of textual prompts and their corresponding images within a unified space. CLIP is pre-trained on a vast dataset which encodes a broad spectrum of concepts [43], making it a versatile choice for a filter, unlike specialized classifiers (e.g., [42]). However, relying on CLIP to identify unacceptable images by solely measuring the distance between the embeddings of a generated image, and an unacceptable concept, was shown not to be robust ([45]). Subsequently, several prior works have identified filtering as a viable direction which needs further exploration [30, 45].

We present a **robust content filter**, ESPRESSO, that identifies unacceptable concepts in generated images using the distance of their embeddings to the text embeddings of *both acceptable and unacceptable concepts*. We project the image embedding onto the vector connecting the text embeddings of acceptable and unacceptable concepts, which makes it harder to generate effective adversarial prompts: the adversary is restricted to adding noise only along this vector, in the direction of the acceptable concept. Fine-tuning ESPRESSO further increases the separation between the text embeddings of acceptable and unacceptable concepts for effectiveness, while maintaining their pairing with their corresponding image embeddings for utility. This fine-tuning approach is further supported by fine-tuning CRTs which show that such an optimization leads to better effectiveness [12, 27, 53]. We claim the following main contributions: we present

- (1) ESPRESSO¹, the **first robust** (CLIP-based) **content filter** which identifies unacceptable concepts by measuring the distance of generated images’ embeddings to the text embeddings of *both* unacceptable and acceptable concepts (Section 4),
- (2) a comprehensive comparative evaluation (Section 5) of the fine-tuned variant of ESPRESSO with six state-of-the-art fine-tuning based CRTs, and one filtering CRT, showing that ESPRESSO is **effective** (~5% CLIP accuracy on unacceptable concepts), **utility-preserving** (~93% normalized CLIP score on acceptable concepts), and **robust** (~4% CLIP accuracy of on adversarial prompts) (Section 6), and

¹We will open-source the code upon publication.

- (3) the **first** approach towards **certifiable robustness of CRTs** by exploring theoretical bounds for certifying the robustness of ESPRESSO, assuming a hypothetically strong adversary, empirical analysis of these bounds, and making the case that ESPRESSO is likely to be more robust in practice. (Section 7).

2 BACKGROUND

We describe T2I models (Section 2.1), different concept removal mechanisms (Section 2.2), and attacks against them (Section 2.3).

2.1 Diffusion based T2I Models

A diffusion based T2I model is a function $f: p \rightarrow x$ which generates an image x for a given a textual prompt p . It comprises two key components: an encoder (ϕ) which is used to incorporate the textual prompt in the image generation process, and a diffusion model (ϵ_θ) which is responsible for the generation of the image.

A popular encoder is CLIP, trained on a large dataset of image-text pairs, to map the embeddings of images and their corresponding text closer together in a joint text-image embedding space [43]. Given N images $\{x_j\}_{j=1}^N$ and their corresponding text prompts $\{p_j\}_{j=1}^N$, the training data is $\mathcal{D} = \{(x_j, p_j)\}_{j=1}^N$.

CLIP is trained to maximize the cosine similarity between the embeddings of a prompt p_j and its corresponding image x_j while minimizing the similarity between p_j and any other x_k for a $k \neq j$. We denote the cosine similarity as $\cos(\phi_p(p_j), \phi_x(x_j))$, where $\phi_x(x_j)$ is the CLIP image embedding of the image x_j , and $\phi_p(p_j)$ is the CLIP text embedding of the prompt p_j . To achieve this, CLIP is trained using a contrastive loss function [29, 54, 61]:

$$\mathcal{L}_{\text{Con}}(\mathcal{D}) = -\frac{1}{N} \sum_{j=1}^N \log \frac{\exp(\cos(\phi_x(x_j), \phi_p(p_j))/\tau)}{\sum_{k=1}^N \exp(\cos(\phi_x(x_j), \phi_p(p_k))/\tau)}$$

where τ is the temperature parameter for scaling the predictions [31, 43].

Given access to a pre-trained encoder ϕ , the actual images in T2I models are generated by a diffusion model, ϵ_θ , parameterized by θ . During training of ϵ_θ , Gaussian noise is added to an initial image x_0 for T time steps to produce x_T , in a process known as the *forward diffusion process*. The noise is then iteratively removed to approximate the initial image \tilde{x}_0 in the *reverse diffusion process*. During inference, the reverse diffusion process generates an image from noise. Further, ϵ_θ can be conditioned with a textual prompt p to guide the generation of \tilde{x}_0 to match the description in p . After generating $\phi_p(p)$, ϵ_θ is trained by minimizing the following loss function: $\mathcal{L} = \mathbb{E}_{\epsilon, \phi_p(p), t} [\|\epsilon - \epsilon_\theta(x_t, \phi_p(p), t)\|_2^2]$ for each time step t , and random Gaussian noise $\epsilon \sim \mathcal{N}(0, 1)$.

Several prominent T2I models (e.g., Stable Diffusion v1.4 (SDv1.4)) improve the efficiency of the diffusion process by conducting it in the embedding space of a variational autoencoder (VAE), rather than on images [46]. For a VAE decoder \mathcal{D} , VAE encoder \mathcal{E} , and $z_t \in \mathcal{E}(x)$ as the latent representation of x in the VAE’s latent space, ϵ_θ is trained by minimizing the following objective: $\mathcal{L} = \mathbb{E}_{\epsilon \sim \mathcal{N}(0,1), z_t \in \mathcal{E}(x), \phi_p(p), t} [\|\epsilon - \epsilon_\theta(z_t, \phi_p(p), t)\|_2^2]$. The final image is generated from the approximation, \tilde{z}_0 , by passing it through \mathcal{D} : $\tilde{x}_0 = \mathcal{D}(\tilde{z}_0)$. Table 1 summarizes frequently used notations.

Table 1: Frequently used notations and their descriptions.

Notation	Description
T2I	Text-to-Image
ϕ	Text encoder (e.g., CLIP)
CRT	Concept Removal Technique
\mathcal{Adv}	Adversary
x	Generated image
x^u	Generated image with unacceptable concept
x^a	Generated image with acceptable concept
$\phi_x(x)$	CLIP embedding for x
x^{adv}	Image generated from adversarial prompt
p	Textual prompt
c^a	Phrase for acceptable concept
c^u	Phrase for unacceptable concept
p^u	Textual prompt containing c^u
p^a	Textual prompt containing c^a
$\phi_p(p)$	CLIP embedding for textual prompt p
p^{adv}	Adversarially generated textual prompt
\mathcal{D}^a	Test dataset with acceptable prompts/images
\mathcal{D}^u	Test dataset with unacceptable prompts/images
\mathcal{D}^a_{val}	Validation dataset with acceptable prompts/images
\mathcal{D}^u_{val}	Validation dataset w/ unacceptable prompts/images
\mathcal{D}^{adv}_{val}	Test dataset with adversarial prompts/images
f	T2I model with CRT where $f: c \rightarrow x$
F	Function for ESPRESSO classifier
α	Regularization parameter for ESPRESSO fine-tuning
τ	Normalization function
ϵ_θ	Diffusion model parameterized by θ
τ	Temperature parameter

2.2 Concept Removal Techniques

The textual phrase for an acceptable concept is c^a , and for an unacceptable concept is c^u . An image x generated from a T2I model may either contain an unacceptable concept (referred to as x^u) or an acceptable one (referred to as x^a). Similarly, a text prompt p may contain a phrase for an acceptable concept (p^a) or an unacceptable concept (p^u). An example of an unacceptable prompt p^u containing an unacceptable concept c^u , *Captain Marvel* is “*Captain Marvel* soaring through the sky”. CRTs seek to thwart the generation of x^u by either fine-tuning the T2I model to suppress x^u , or using a classifier as a filter to detect x^u . We first present six state-of-the-art fine-tuning CRTs:

Concept Ablation (CA) [27] fine-tunes the T2I model to minimize the KL divergence between the model’s output for p^u and p^a to force the generation of x^a instead of x^u . Formally, they optimize the following objective function:

$$\mathcal{L}_{CA} = \mathbb{E}_{\epsilon, z_t, c^u, c^a, t} [w_t \|\epsilon_\theta(z_t, \phi_p(p^a), t).sg() - \epsilon_\theta(z_t, \phi_p(p^u), t)\|_2^2]$$

where $\epsilon \sim \mathcal{N}(0, 1)$, $z_t \in \mathcal{E}$, and w_t is a time-dependent weight, and $.sg()$ is the stop-gradient operation.

Forget-Me-Not (FMN) [64] minimizes the activation maps for c^u by modifying ϵ_θ ’s cross-attention layers. Further, fine-tuning ϵ_θ , instead of just the cross-attention layers, results in degraded utility.

Selective Amnesia (SA) [18] fine-tunes T2I models by adapting continuous learning techniques (elastic weight consolidation and generative replay) for T2I models to forget a concept. They optimize $\mathbb{P}(x|\theta^*, c^u)$, the probability of generating x given θ^* and c^u , where θ^* are the frozen parameters of the original T2I model:

$$\mathcal{L}_{SA} = -\mathbb{E}_{\mathbb{P}(x|p)\mathbb{P}_f(c^u)} [\log \mathbb{P}(x|\theta^*, c^u)] - \lambda \sum_i \frac{M_i}{2} (\theta_i^* - \theta_i)^2 + \mathbb{E}_{\mathbb{P}(x|p)\mathbb{P}_f(c^a)} [\log \mathbb{P}(x|\theta, c^a)]$$

where M is the Fisher information matrix over c^a and c^u , \mathbb{P}_r and \mathbb{P}_f are probabilities taken over the distributions of c^a and c^u respectively, and λ is a regularization parameter.

Erased Stable Diffusion (ESD) [13] fine-tunes the T2I model by modifying the reverse diffusion process to reduce the probability of generating x^u :

$$\epsilon_{\theta}(x_t, \phi_p(c^u), t) = \epsilon_{\theta^*}(x_t, t) + \eta(\epsilon_{\theta^*}(x_t, \phi_p(c^u), t) - \epsilon_{\theta^*}(x_t, t))$$

where $\eta > 0$ encourages the noise conditioned on c^u to match the unconditioned noise.

Unified Concept Editing (UCE) [16] fine-tunes the T2I model’s cross-attention layers with the help of a language model to minimize the influence of c^u , while keeping the influence of remaining concepts unchanged. Their fine-tuning objective is

$$\mathcal{L}_{UCE} = \sum_{c^u \in C^u, c^a \in C^a} \|Wc^u - W^{\text{old}}c^a\|_2^2 + \sum_{c \in S} \|Wc - W^{\text{old}}c\|_2^2$$

where W, W^{old} are the parameters of the fine-tuned and original cross-attention layers in ϵ_{θ} , C^u and C^a are the space over some pre-defined unacceptable and acceptable concepts, and S is a set of concepts for which to preserve utility.

Safe diffusion (SDD) [23] fine-tunes the T2I model by encouraging the diffusion model noise conditioned on c^u to match the unconditioned noise, while minimizing the utility drop using the following objective function:

$$\mathcal{L}_{SDD} = \mathbb{E}_{\epsilon \sim \mathcal{N}(0,1), z_t \in \mathcal{E}, c^u, t} [\|\epsilon_{\theta}(z_t, \phi_p(c^u), t) - \epsilon_{\theta}(z_t, t).sg(\cdot)\|_2^2]$$

We now describe two filtering CRTs:

Stable Diffusion Filter (SD-Filter) [43] is black-box and the design of the filter is not publicly available. However, Rando et al. [45] hypothesize that it involves computing the cosine similarity between the embeddings of a generated image, x , and a pre-defined set of c^u . If the cosine similarity is greater than some threshold (Γ), then the unacceptable concept is detected. Formally, their filter F_{SD} can be described as

$$F_{SD}(x) = \begin{cases} 1 & \cos(\phi_x(x), \phi_p(c^u)) > \Gamma \\ 0 & \text{otherwise} \end{cases}$$

where $\cos(\phi_x(x), \phi_p(c^u)) = \overline{\phi_x(x)} \cdot \overline{\phi_p(c^u)}$, and $\bar{\cdot}$ denotes normalization. Here $F_{SD}(x) = 1$ indicates x^a and $F_{SD}(x) = 0$ indicates x^u . Note that Γ is possibly different for different c^u .

Unsafe Diffusion (UD) [42] is the current state-of-the-art filtering CRT which trains a multi-headed neural network classifier on top of CLIP to identify x^u . The different heads for the neural network are for classifying different c^u : *nudity, violence, disturbing, hateful, and political*. Their objective is given as $F_{UD}(x) = \text{MLP}(\phi_x(x))$ where MLP is a multi-layer perceptron, and $F_{UD} \in \{0, 1\}$.

2.3 Evading Concept Removal Techniques

An adversary ($\mathcal{A}dv$) may generate adversarial prompts (p^{adv}) to evade CRTs and force the T2I model to generate unacceptable images. We denote a dataset containing adversarial prompts and their corresponding images as $\mathcal{D}_{adv}^u = \{(x_j^{adv}, p_j^{adv})\}_{j=1}^N$. $\mathcal{A}dv$ is assumed to account for the target T2I model, f , using a CRT. A dumb $\mathcal{A}dv$ who does not account for this is *naive*. All these attacks generate p^{adv} as an optimization problem using some reference x^u (or

the difference between p^a and p^u) as the ground truth. Different attacks vary in ways to solve this optimization. We present four state-of-the-art attacks below:

PEZ [57] generates p^{adv} by identifying text tokens which minimize the following objective function: $\mathcal{L}_{PEZ} = 1 - \cos(\phi_p(p^{adv}), \phi_x(x^u))$.

RingBell [53] uses a genetic algorithm to identify tokens for p^{adv} by minimizing the difference between the embedding vectors of p^u and p^a : $\phi_p(\hat{p}) = \frac{1}{N} \sum_{i=1}^N \{\phi_p(p_i^u) - \phi_p(p_i^a)\}$ from a set of N prompts. The optimization can be formulated as: $\min_{p^{adv}} \|\phi_p(p^{adv}) - (\phi_p(p^{init}) + \eta \cdot \phi_p(\hat{p}))\|^2$ where p^{init} is an initial target prompt which is modified into p^{adv} . Further, the optimization relies on a fitness function using mean-squared error: $\mathcal{L}_{RingBell} = \mathcal{L}_{MSE}(\phi_p(c^u), \phi_p(p^{adv}))$ where c^u is a prompt that generates x^u in a T2I model.

SneakyPrompt [63] uses reinforcement learning to generate p^{adv} specifically against filtering CRTs. Given an initial prompt p^{init} , the attack searches for tokens to update p^{init} to form p^{adv} . The reward function is the cosine similarity between $\phi_x(x^{adv})$ and $\phi_p(p^{adv})$, where x^{adv} is the generated image corresponding to p^{adv} . Typically, we use p^u as p^{init} to improve effectiveness and achieve faster convergence.

CCE [38] uses textual-inversion to generate p^{adv} [11]. $\mathcal{A}dv$ updates CLIP’s vocabulary to include a token new “<s>” which, when included in p^{adv} , generates $\mathcal{A}dv$ ’s desired image. To optimize <s>, we find v , an embedding for <s>, corresponding to least loss $\mathcal{L}_{CCE} = \mathcal{L}_{MSE}(\epsilon, \epsilon_{\theta}(z_t, v, t))$, where $\epsilon \sim \mathcal{N}(0, 1)$.

All of these attacks are naive except for CCE and SneakyPrompt, which account for different fine-tuning CRTs. In Section 5.1, we describe how we modify these naive attacks to account for CRTs.

3 PROBLEM STATEMENT

Our goal is to design a CRT which can effectively detect unacceptable concepts in images generated from T2I models. We describe an adversary model, requirements of an ideal CRT, and limitations of prior works according to the requirements.

Adversary Model. We assume (blackbox) access to a deployed target T2I model (f) to which a client can send an input (p) to generate an image (x). Further, f uses some CRT. The goal of the adversary ($\mathcal{A}dv$) is to force f to generate an image containing an unacceptable concept (x^u) despite the presence of a CRT to suppress it. We give an advantage to $\mathcal{A}dv$ by allowing whitebox access to a local identical copy of f with the CRT for use in designing attacks. This is reasonable as ϵ_{θ} and CLIP are publicly available. For filtering-based CRTs, we assume that $\mathcal{A}dv$ has whitebox access to the filter, enabling them to use its loss function in designing the attacks.

Requirements An ideal CRT should be: **R1 Effective** in minimizing the generation of images with unacceptable concepts (x^u); **R2 Utility-preserving**, maintaining the quality of acceptable images (for fine-tuning CRTs) or not blocking them (for filtering CRTs); and **R3 Robust** to resist evasion with adversarial prompts (p^{adv}).

Limitations of Prior Works. In Section 6, we empirically show the limitations of prior works by evaluating **R1**, **R2**, and **R3** of different CRTs. We provide a brief summary here. *Fine-tuning* CRTs [13, 16, 18, 18, 23, 27, 64] modify f thereby explicitly creating a trade-off between effectiveness (**R1**) and utility (**R2**). Further, these CRTs do not consider robustness (**R3**) in their design and hence, are

susceptible to evasion by $\mathcal{A}dv$ using p^{adv} . Filtering CRTs [42, 43] detect unacceptable concepts either in p (aka prompt filter) or in x and block them (a.k.a image filter). Since, they do not modify f , they can maintain utility without impacting effectiveness. Prior filtering approaches may not be accurate in detecting unacceptable concepts (impacts **R1**) [30]. They can also be easily evaded (harms **R3**) ([45] and Section 6.2). Further, the current state-of-the-art filter, UD [42], trains specialized classifiers for each concept on substantial data, which limits their generalization to new concepts.

4 ESPRESSO: ROBUST FILTERING CRT

We present ESPRESSO, a robust **concept filtering** CRT which satisfies all the requirements from Section 3. ESPRESSO uses a classifier to detect images with unacceptable concepts. We identify CLIP as the natural choice for such a classifier as it is (1) pre-trained on a large dataset covering a wide range of concepts, and (2) used across many T2I models, and encodes similar information as seen in these models. Hence, CLIP is a better choice for a filter than training specialized classifiers to identify specific concepts (e.g., [42]).

However, simply using CLIP for ESPRESSO is not sufficient as seen in Stable Diffusion’s filter [43] F_{SD} . Here, the filter thresholds the cosine similarity between the embeddings of x and each pre-defined unacceptable concept to identify x^u . Rando et al. [45] design adversarial prompts (p^{adv}) to evade F_{SD} . As F_{SD} uses only the cosine similarity to c^u , it gives $\mathcal{A}dv$ the freedom to modify the prompt embeddings in *any direction* while optimizing for p^{adv} , to force a misclassification. We address this in ESPRESSO to ensure effectiveness and robustness while maintaining utility by (a) modifying CLIP’s classification objective for **R1** and **R3**, and (b) fine-tuning to further improve ESPRESSO.

Modifying CLIP’s Classification Objective. We modify the objective function of ESPRESSO for filtering by using the cosine similarity to both c^a and c^u instead of just the cosine similarity to c^u . Further, as observed in prior fine-tuning CRTs, jointly optimizing for two embeddings yields better effectiveness and utility [12, 27, 53]. Using the modified classification objective, we restrict $\mathcal{A}dv$ to adding noise only along the low-dimensional vector joining c^a and c^u , in the direction of c^a . This is more challenging for $\mathcal{A}dv$ to evade than F_{SD} , as projecting to a lower-dimensional representation can improve robustness [3, 56].

Given x , ESPRESSO checks the cosine similarity of $\phi_x(x)$ to $\phi_p(c^u)$ and $\phi_p(c^a)$. Formally, we define ESPRESSO as $F(x, c^u, c^a)$

$$= \operatorname{argmax}_i \left(\left\{ \frac{\exp(\cos(\phi_x(x), \phi_p(c_i))/\tau)}{\sum_{j \in \{a,u\}} \exp(\cos(\phi_x(x), \phi_p(c_j))/\tau)} \right\}_{i \in \{a,u\}} \right) \quad (1)$$

where $\tau = \frac{1}{100}$ is the default temperature parameter used in CLIP. Further, the cosine similarity is equivalent to the scaled Euclidean distance between the embeddings [31]:

$$\begin{aligned} (\overline{\phi_x(x)} - \overline{\phi_p(c)})^T (\overline{\phi_x(x)} - \overline{\phi_p(c)}) &= 2 - 2\overline{\phi_x(x)} \cdot \overline{\phi_p(c)} \\ \implies \cos(x, c) &= \frac{-1}{2} (\overline{\phi_x(x)} - \overline{\phi_p(c)})^T (\overline{\phi_x(x)} - \overline{\phi_p(c)}) + 1 \end{aligned}$$

Hence, by using CLIP as a filter, we project the image embeddings onto the vector between c^u and c^a and classify it based on its distance to both.

Fine-tuning. We conjecture that we can further improve ESPRESSO by maximizing the distance between $\phi_p(p^u)$ and $\phi_p(p^a)$. In other words, we can fine-tune F to minimize the following loss function:

$$L_{\text{ESPRESSO}} = -\|\overline{\phi_p(p^u)} - \overline{\phi_p(p^a)}\|_2 \quad (2)$$

For the case where p^u and p^a are opposites (e.g., they contain *violence* and *peaceful*), the above objective function might result in a low correlation between $\phi_p(p)$ and the corresponding $\phi_x(x)$. This might result in poor utility. We account for this by using the following objective function instead:

$$\begin{aligned} \mathcal{L}_{\text{ESPRESSO}} &= \alpha_{aa} \mathcal{L}_{\text{Con}}(\mathcal{D}_{aa}) - \alpha_{ua} \mathcal{L}_{\text{Con}}(\mathcal{D}_{ua}) \\ &+ \alpha_{uu} \mathcal{L}_{\text{Con}}(\mathcal{D}_{uu}) - \alpha_{au} \mathcal{L}_{\text{Con}}(\mathcal{D}_{au}) \\ &+ \alpha_{uu-t} \mathcal{L}_{\text{MSE}}(\phi_p(\mathcal{P}^u), \phi_p(\mathcal{P}^a)) \end{aligned} \quad (3)$$

where $\mathcal{D}_{aa} = \{(x^a_j, p^a_j)\}_{j=1}^N$, $\mathcal{D}_{au} = \{(x^a_j, p^u_j)\}_{j=1}^N$, $\mathcal{D}_{ua} = \{(x^u_j, p^a_j)\}_{j=1}^N$, $\mathcal{D}_{uu} = \{(x^u_j, p^u_j)\}_{j=1}^N$, $\mathcal{P}^u = \{p^u_j\}$, and $\mathcal{P}^a = \{p^a_j\}$, and α are regularization hyperparameters. We assign equal weight to each of the loss terms, thus choosing $\alpha_{(\cdot)} = 1$. The above objective function encourages the CLIP embeddings of x^u and p^u , and x^a and p^a , to be closer together while increasing the distance between x^u and p^a , and x^a and p^u , respectively. During fine-tuning of ESPRESSO, there is a trade-off between effectiveness and utility which is inherent to all other fine-tuning CRTs as well. We subject our fine-tuning to the constraint that achieved the highest effectiveness for the least drop in utility.

We use prompts for fine-tuning in Equation (2) and Equation (3) instead of only concepts. This is because p^u and p^a , containing c^u and c^a , provide more context.

The prompts used for the T2I model are not known before-hand, but we can define the concepts to be filtered. Since the prompt includes these concepts, filtering the images generated from the prompts is sufficient.

Replacement of Blocked Images. As with other filters, on detecting an image with an unacceptable concept, ESPRESSO generates a replacement image as in SDv1.4 [43].

5 EXPERIMENTAL SETUP

We describe the baselines for CRTs and attacks (Section 5.1), different concepts used for evaluation (Section 5.2), dataset and model configuration (Section 5.3), and metrics (Section 5.4).

5.1 Evaluation Baselines

We compare ESPRESSO with prior state-of-the-art CRTs across **R1**, **R2**, and **R3**. We use six fine-tuning CRTs (CA, FMN, SA, ESD, UCE, and SDD) and one filtering CRT (UD) which are described in Section 2.2.

To evaluate **R3**, we consider different state-of-art attacks from literature (Section 2.3). We modify (indicated with “+”) existing naïve attacks, Ring-a-Bell, and PEZ, to account for CRTs. The CRTs use some variant of the following optimization: detach c^u from p such that the generated image is far from c^u and closer to some c^a . Hence, to design an effective attack which accounts for such CRTs, in addition to the attacks’ original objectives, we minimize the loss between p^{adv} and c^a while increasing its loss with c^u . This, in turn, will move $\phi_p(p^{adv})$ closer to $\phi_p(c^u)$ and further from $\phi_p(c^a)$. We

modify the attacks by considering the following loss function:

$$\mathcal{L}_{att+} = \mathcal{L}_{att} - \alpha_u \mathcal{L}_{MSE}(\phi_p(c^u), \phi_p(p^{adv})) + \alpha_a \mathcal{L}_{MSE}(\phi_p(c^a), \phi_p(p^{adv})) \quad (4)$$

where $att \in \{\text{RingBell}, \text{PEZ}\}$ when $\text{CRT} \in \{\text{CA}, \text{FMN}, \text{SA}, \text{ESD}, \text{UCE}, \text{SDD}, \text{UD}, \text{ESPRESSO}\}$, and \mathcal{L}_{att} is from Section 2.2. Recall from Section 2.3 that CCE already accounts for different fine-tuning CRTs. For UD and ESPRESSO, we use Equation 4. We assign equal weight to all loss terms and use $\alpha_u = \alpha_a = 1$. We call this variant CCE+.

The typographic attack [37] against CLIP is where text characters are superimposed onto an (unrelated) image to fool CLIP by forcing it to focus on the this text instead of the image. We turn this into an attack against CRTs by superimposing c^a at the bottom of x^u . Using the resulting adversarial images, we use PEZ+ to find their corresponding p^{adv} s. We call this attack *Typo+*.

5.2 Concepts

Concept Types. We use the same set of unacceptable concepts as in prior work [23, 27, 38], categorizing them into three groups:

- Group-1 covers inappropriate concepts such as *nudity* (e.g., female breasts or male/female genitalia), *violence* (e.g., bloody scenes, fighting, burning, hanging, weapons, and wars), *disturbing* (e.g., distorted faces, bodies, human flesh, or bodily fluids), and *hateful* (e.g., defamatory depictions of races, harmful stereotypes, or Holocaust scenes).
- Group-2 covers copyright-infringing concepts such as *Grumpy Cat*, *Nemo*, *Captain Marvel*, *Snoopy*, and *R2D2*.
- Group-3 covers (unauthorized) use of personal images for celebrities such as *Taylor Swift*, *Angelina Jolie*, *Brad Pitt*, and *Elon Musk*.

Table 2: Summary of unacceptable concepts (c^u), acceptable concepts (c^a), and whether we use them to evaluate fine-tuning CRTs, filtering CRTs, or both.

Type	$c^u \rightarrow c^a$	CRT (s)
Group-1	<i>Nudity</i> \rightarrow <i>Clean</i>	Both
	<i>Violence</i> \rightarrow <i>Peaceful</i>	Both
	<i>Disturbing</i> \rightarrow <i>Pleasing</i>	Filtering
	<i>Hateful</i> \rightarrow <i>Loving</i>	Filtering
Group-2	<i>Grumpy Cat</i> \rightarrow <i>Cat</i>	Fine-tuning
	<i>Nemo</i> \rightarrow <i>Fish</i>	Fine-tuning
	<i>Captain Marvel</i> \rightarrow <i>Female Superhero</i>	Fine-tuning
	<i>Snoopy</i> \rightarrow <i>Dog</i>	Fine-tuning
	<i>R2D2</i> \rightarrow <i>Robot</i>	Fine-tuning
Group-3	<i>Taylor Swift</i> \rightarrow <i>Woman</i>	Fine-tuning
	<i>Angelina Jolie</i> \rightarrow <i>Woman</i>	Fine-tuning
	<i>Brad Pitt</i> \rightarrow <i>Man</i>	Fine-tuning
	<i>Elon Musk</i> \rightarrow <i>Man</i>	Fine-tuning

Identifying Acceptable Concepts. We specify a matching c^a for every c^u so that CRTs can steer away from generating c^u concepts and instead focus on c^a . We indicate “ $c^u \rightarrow c^a$ ” for each group and discuss our choice of c^a .

- Group-1: c^a is the opposite of c^u , except for *nudity*. For instance, *violence* \rightarrow *peaceful*, *disturbing* \rightarrow *pleasing*, and *hateful* \rightarrow *loving*. For *nudity*, we compared *clothed* with *clean* on a separate validation dataset (c.f. Section 5.3 and Table 4), and eliminated *clothed* because it blocked images with minimal exposed skin despite being acceptable [42, 49]. Similarly, we evaluated and eliminated

alternatives of c^a for *violence* (*nonviolent*, and *gentle*), *disturbing* (*calming*, and *soothing*), and *hateful* (*compassionate*, and *kind*).

- Group-2: c^a is the type of c^u , taken from prior works [13, 18, 27]. For instance, *Grumpy Cat* \rightarrow *cat*, *Nemo* \rightarrow *fish*, *Captain Marvel* \rightarrow *female superhero*, *Snoopy* \rightarrow *dog*, and *R2D2* \rightarrow *robot*.
- Group-3: c^a is the gender of c^u , taken from prior works [18, 23, 64]. For instance, *{Taylor Swift, Angelina Jolie}* \rightarrow *woman* and *{Brad Pitt, Elon Musk}* \rightarrow *man*.

Selecting Concepts to Evaluate CRTs. Different prior works used different concepts in their evaluation. Filtering CRTs were evaluated on inappropriate concepts in Group-1 while fine-tuning CRTs were evaluated on *nudity* and *violence* from Group-1, and all the concepts from Group-2 and Group-3. Hence, we compare ESPRESSO with each CRT category separately using concepts they were evaluated on. We summarize all the concepts used for evaluation in Table 2.

5.3 Dataset and Model Configurations

Training/Fine-tuning Datasets. We summarize the configuration for training/fine-tuning datasets in Table 3.

Table 3: Training dataset configurations required by CRTs.

CRT	Configuration Requirements
CA [27]	200 unacceptable prompts (p^a) from ChatGPT with one image/prompt from SDv1.4
ESD [13]	Unacceptable concept (c^u)
FMN [64]	8 unacceptable prompts (p^u) and one image/prompt from SDv1.4
SDD [23]	Unacceptable concept (c^u) and 10 corresponding images
SA [18]	Acceptable concept (c^a) and 1000 corresponding images, and 6 unacceptable prompts (p^u)
UCE [16]	Unacceptable and acceptable concepts (c^u and c^a)
UD [42]	776 total images with 580 acceptable images (x^a), and 196 unacceptable images (x^u): <i>nudity</i> (48), <i>violence</i> (45), <i>disturbing</i> (68), and <i>hateful</i> (35)
ESPRESSO	10 unacceptable prompts (p^u) and acceptable prompts (p^a) using ChatGPT with one image/prompt from SDv1.4

Fine-tuning CRTs. Different fine-tuning CRTs use different dataset configurations to ensure that **R1** and **R2** are met. We use the exact same configuration as described in each of the prior works to ensure that they satisfy the requirements claimed in their papers. While the configuration across different CRTs vary, the configuration for a specific CRT across different concepts is the same, in accordance with the instructions in the respective works. We briefly summarize them in Table 3. CA uses acceptable prompts which are generated from ChatGPT such that they contain c^a , and 1 image per prompt. ESD and SDD both use an unacceptable concept, and SDD additionally uses 10 images corresponding to c^u . All images are generated using SD v1.4. FMN uses unacceptable prompts of the form “An image of $\{c^u\}$ ”, and 1 image per prompt. For all the fine-tuning CRTs, we use their publicly available code for training to ensure the configuration is same as reported in their papers [14, 15, 17, 24, 28, 41, 65].

Filtering CRTs. We train F_{UD} using its exact dataset configuration (Table 3) and code [42]. For ESPRESSO, we follow the template by Kumari et al. [27] to generate 10 unacceptable and acceptable prompts using ChatGPT, with one image per prompt from SDv1.4. For Group-2 concepts, we randomly select 10 ChatGPT-generated prompts from the datasets provided by Kumari et al. [27]. Our choice for having a small amount of training data is inspired from prior works

on poisoning attacks which show that little data is required to modify CLIP [5, 61]. Our results also show that using such little data is indeed sufficient to meet **R1**, **R2**, and **R3** (c.f. Section 6).

Validation Datasets. For **R1**, we generate 10 unacceptable prompts using ChatGPT, and generate 5 images per prompt using SD v1.4. We denote this validation dataset as \mathcal{D}_{val}^u . For **R2**, we randomly chose 100 non-overlapping acceptable prompts from the COCO 2014 dataset [32], and 1 image per prompt, generated from SD v1.4. We denote this validation dataset as \mathcal{D}_{val}^a . We summarize in Table 4.

Table 4: Configuration for Validation Datasets.

Concepts	Dataset	Configuration Requirements
Group-1	\mathcal{D}_{val}^u	10 unacceptable prompts (p^u) from ChatGPT and 5 images (x^u) per prompt from SDv1.4
Group-2	\mathcal{D}_{val}^u	10 unacceptable prompts (p^u) from ChatGPT and 5 images (x^u) per prompt from SDv1.4
Group-3	\mathcal{D}_{val}^u	10 unacceptable prompts (p^u) from ChatGPT and 5 images (x^u) per prompt from SDv1.4
All	\mathcal{D}_{val}^a	100 acceptable prompts (p^a) and 1 image (x^a) per prompt from the COCO 2014 dataset

Evaluation Datasets. We now describe the test datasets for evaluation: test dataset with acceptable prompts is $\mathcal{D}_{te}^a = \{(x^a_j, p^a_j)\}_{j=1}^N$ and with unacceptable prompts is $\mathcal{D}_{te}^u = \{(x^u_j, p^u_j)\}_{j=1}^N$.

For Group-1, we use an independent benchmark dataset, Inappropriate Image Prompts (I2P), containing prompts likely to generate unsafe images [49]. It covers all four Group-1 concepts. For *nudity*, I2P includes a “nudity percentage” attribute. We choose all unacceptable prompts with a nudity percentage > 10 , resulting in a total of 300 unacceptable prompts, in accordance with prior works [13, 16]. UD [42] also used *political* as a concept, which is excluded from our evaluation since it is not a part of I2P. Note that I2P prompts do not explicitly contain the unacceptable concepts, i.e., the words *nude*, *violent*, *hateful*, or *disturbing*. For Group-2 and Group-3 concepts, there are no standard benchmark datasets. Hence, we generate the dataset by following prior works [13, 27] to obtain 200 unacceptable images, x^u , generated from SDv1.4 from 10 unacceptable prompts, p^u , generated from ChatGPT. These datasets constitute \mathcal{D}_{te}^u . For utility, we use the COCO 2014 test dataset (\mathcal{D}_{te}^a) with 200 randomly chosen acceptable prompts. This dataset constitutes \mathcal{D}_{te}^a . We summarize these datasets in Table 5.

Table 5: Configuration for Evaluation Datasets.

Concepts	Dataset	Configuration Requirements
Group-1	\mathcal{D}_{te}^u	I2P Dataset [49] of unacceptable prompts: for <i>nudity</i> : 449 prompts, <i>violence</i> : 758, <i>disturbing</i> : 857, <i>hateful</i> : 235
Group-2	\mathcal{D}_{te}^u	10 unacceptable prompts (p^u) from ChatGPT and 20 images (x^u) per prompt from SDv1.4
Group-3	\mathcal{D}_{te}^u	10 unacceptable prompts (p^u) from ChatGPT and 20 images (x^u) per prompt from SDv1.4
All	\mathcal{D}_{te}^a	200 acceptable prompts (p^a) from COCO 2014 dataset

5.4 Metrics

We now describe the metrics to evaluate each of the requirements. We assume access to a *reference CLIP*, separate from those used in CRTs and f . This is a standard assumption in prior works to compute different metrics [16, 19, 23, 27].

R1 (Effectiveness). Depending on the CRT, we use:

- **CLIP accuracy** [19, 27] for fine-tuning CRTs. This is the cosine similarity (divided by the temperature parameter τ) between the embeddings of the generated image x with the embeddings of c^u and c^a from the reference CLIP, where τ is the temperature parameter of the reference CLIP, $\frac{1}{100}$. This outputs the likelihood of predicting c^u . Hence, CLIP accuracy should be low (ideally zero) for effective concept removal. Formally, it is:

$$\frac{\exp(\cos(\tilde{\phi}_x(x), \tilde{\phi}_p(c^u)/\tau))}{\exp(\cos(\tilde{\phi}_x(x), \tilde{\phi}_p(c^u)/\tau)) + \exp(\cos(\tilde{\phi}_x(x), \tilde{\phi}_p(c^a)/\tau))}$$

where $\tilde{\phi}_p$ and $\tilde{\phi}_x$ are embeddings from the reference CLIP. If ESPRESSO detects x^u , a replacement image is generated. We calculate the CLIP accuracy on the final set of images after filtering. Since the metrics compare with baseline reference CLIP, we use the same default replacement image as in the SD v1.4 filter.

- **False Negative Rates (FNR)** [42, 45] for filtering CRTs is the fraction of images with c^u which are not blocked. It should be low (ideally zero).

R2 (Utility). Depending on the CRT, we use:

- **Normalized CLIP score** for fine-tuning CRTs, which is the ratio of cosine similarity (scaled by $\frac{1}{\tau}$, where $\tau = \frac{1}{100}$) between $\phi_x(x)$ and $\phi_p(p)$ from f compared to that from a reference CLIP as a baseline. Formally, $\frac{\cos(\phi_x(x), \phi_p(p))/\tau}{\cos(\tilde{\phi}_x(x), \tilde{\phi}_p(p))/\tau}$. Normalized CLIP score should be high (ideally one) for high utility. This metric is different from standard CLIP score from prior work [16, 19, 23, 27] which measures the cosine similarity between $\phi_x(x)$ and $\phi_p(p)$ from f . Normalizing the CLIP score helps compare f to the reference CLIP which has the maximum achievable CLIP score.
- **False Positive Rates (FPR)** [42, 45] for filtering CRTs is the fraction of images without c^u which are blocked. It should be low (ideally zero).

R3 (Robustness). We use the same metrics as effectiveness: CLIP accuracy to evaluate fine-tuning CRTs and compare ESPRESSO with them, and FNR for filtering CRTs. However, we compute both the metrics on \mathcal{D}_{adv}^u .

6 EVALUATION

We now evaluate ESPRESSO, first comparing with fine-tuning CRTs (Section 6.1), followed by filtering CRT (Section 6.2).

6.1 Comparison with Fine-tuning CRTs

R1 Effectiveness. We report CLIP accuracy in Table 6 for all eleven concepts on \mathcal{D}_{te}^u .

All CRTs show poor accuracy on *nudity* and *violence*. We attribute this to fine-tuning CRTs being sensitive to the input prompts [33, 39, 62]. Hence, they perform poorly for *nudity* and *violence* which do not explicitly contain unacceptable concepts. In comparison to other CRTs, ESPRESSO consistently maintains high accuracy on the I2P benchmark dataset as it classified based on the generated images and not prompts. Further, ESPRESSO satisfies **R1** using only 20 prompts and corresponding images for training. This is consistent with results on CLIP poisoning where changing the performance of CLIP only required a small number of poison samples [5, 61].

Table 6: R1 Effectiveness: Comparison with fine-tuning CRTs using CLIP accuracy on *unacceptable* prompts (lower is better). We use **red if accuracy is >50; **blue** if accuracy is between 25-50; **green** if accuracy is <25.**

CRT	Concepts										
	Nudity (I2P)	Violence (I2P)	Grumpy Cat	Nemo	Captain Marvel	Snoopy	R2D2	Taylor Swift	Angelina Jolie	Brad Pitt	Elon Musk
CA [27]	0.82 ± 0.01	0.78 ± 0.01	0.00 ± 0.00	0.02 ± 0.00	0.40 ± 0.05	0.06 ± 0.05	0.13 ± 0.02	0.73 ± 0.05	0.83 ± 0.02	0.86 ± 0.04	0.64 ± 0.03
FMN [64]	0.83 ± 0.01	0.64 ± 0.04	0.34 ± 0.02	0.61 ± 0.01	0.82 ± 0.03	0.16 ± 0.00	0.89 ± 0.03	0.45 ± 0.02	0.59 ± 0.06	0.79 ± 0.04	0.56 ± 0.22
SA [18]	0.69 ± 0.09	0.69 ± 0.00	0.16 ± 0.00	0.87 ± 0.04	0.93 ± 0.02	0.55 ± 0.07	0.98 ± 0.01	0.82 ± 0.05	0.49 ± 0.04	0.63 ± 0.05	0.75 ± 0.04
ESD [13]	0.62 ± 0.06	0.63 ± 0.01	0.28 ± 0.06	0.64 ± 0.06	0.37 ± 0.04	0.20 ± 0.02	0.41 ± 0.04	0.11 ± 0.02	0.29 ± 0.05	0.17 ± 0.02	0.17 ± 0.02
UCE [16]	0.70 ± 0.01	0.71 ± 0.01	0.05 ± 0.00	0.43 ± 0.00	0.04 ± 0.00	0.03 ± 0.00	0.40 ± 0.01	0.02 ± 0.01	0.06 ± 0.00	0.05 ± 0.00	0.10 ± 0.01
SDD [23]	0.57 ± 0.02	0.55 ± 0.02	0.20 ± 0.02	0.20 ± 0.03	0.41 ± 0.03	0.37 ± 0.03	0.39 ± 0.02	0.05 ± 0.02	0.06 ± 0.01	0.04 ± 0.01	0.06 ± 0.01
ESPRESSO	0.15 ± 0.06	0.20 ± 0.05	0.00 ± 0.01	0.10 ± 0.02	0.03 ± 0.01	0.08 ± 0.02	0.00 ± 0.00	0.02 ± 0.00	0.03 ± 0.00	0.00 ± 0.00	0.03 ± 0.00

Table 7: R2 (Utility): Comparison with fine-tuning CRTs using normalized CLIP scores on *acceptable* prompts (higher is better). We use **red if score is between 50-70, **blue** if between 70-90; **green** if >90.**

CRT	Concepts										
	Nudity	Violence	Grumpy Cat	Nemo	Captain Marvel	Snoopy	R2D2	Taylor Swift	Angelina Jolie	Brad Pitt	Elon Musk
CA [27]	0.93 ± 0.00	0.93 ± 0.00	0.93 ± 0.00	0.93 ± 0.00	0.93 ± 0.00	0.93 ± 0.00	0.93 ± 0.00	0.93 ± 0.00	0.93 ± 0.00	0.93 ± 0.00	0.93 ± 0.00
FMN [64]	0.79 ± 0.00	0.79 ± 0.00	0.79 ± 0.00	0.79 ± 0.00	0.79 ± 0.00	0.79 ± 0.00	0.79 ± 0.00	0.79 ± 0.00	0.79 ± 0.00	0.79 ± 0.00	0.79 ± 0.00
SA [18]	0.79 ± 0.00	0.79 ± 0.00	0.79 ± 0.00	0.79 ± 0.00	0.79 ± 0.00	0.79 ± 0.00	0.79 ± 0.00	0.79 ± 0.00	0.79 ± 0.00	0.79 ± 0.01	0.79 ± 0.00
ESD [13]	0.82 ± 0.01	0.82 ± 0.00	0.82 ± 0.01	0.82 ± 0.00	0.82 ± 0.01	0.82 ± 0.01	0.82 ± 0.01	0.82 ± 0.01	0.82 ± 0.01	0.82 ± 0.01	0.82 ± 0.01
UCE [16]	0.96 ± 0.02	0.96 ± 0.00	0.97 ± 0.03	0.96 ± 0.00	0.96 ± 0.00	0.97 ± 0.02	0.96 ± 0.00	0.97 ± 0.02	0.97 ± 0.01	0.96 ± 0.03	0.97 ± 0.00
SDD [23]	0.86 ± 0.00	0.75 ± 0.00	0.93 ± 0.00	0.86 ± 0.00	0.82 ± 0.00	0.82 ± 0.00	0.64 ± 0.00	0.82 ± 0.00	0.82 ± 0.00	0.61 ± 0.00	0.89 ± 0.00
ESPRESSO	0.94 ± 0.08	0.59 ± 0.11	0.98 ± 0.04	0.37 ± 0.02	0.37 ± 0.03	0.66 ± 0.03	0.66 ± 0.02	0.98 ± 0.02	0.98 ± 0.03	0.98 ± 0.01	0.97 ± 0.01

ESD, UCE, and SDD have better accuracy compared to the other three fine-tuning CRTs. This could be attributed to the similar optimizations used by ESD and SDD for fine-tuning the T2I model. Both ESD and SDD fine-tune ϵ_θ , conditioned on c^u , to match original ϵ_θ without any prompt to reduce the influence of c^u on the output. For UCE, the reason for its higher effectiveness might be because it directly removes the influence of c^u from the weights of T2I.

R2 Utility. We report normalized CLIP scores in Table 7 on \mathcal{D}_{te}^a .

All the fine-tuning CRTs perform well across all concepts (either **blue** or **green**). This could be attributed to fine-tuning while explicitly including utility preservation as a requirement. We observe that CA with KL-Divergence-based optimization targeted for cross-attention layers, and UCE with a precise closed-form solution to model updates, preserve utility better than other CRTs.

ESPRESSO achieves high utility preservation for all concepts except for *violence*, and some Group-2 concepts (*Nemo*, *Captain Marvel*, *Snoopy*, and *R2D2*). During fine-tuning, effectiveness improves but at the cost of utility, which is inherent to all fine-tuning CRTs. For *violence*, in our experiments, we observed an early decrease in utility during the very first epoch resulting in poor trade-off between effectiveness and utility preservation. We attribute the poor utility preservation on Group-2 concepts to the ambiguity in the unacceptable concepts. For instance, *Nemo* is both a fish and a ship captain [55], and *Captain Marvel* represents both a male and a female superhero [10]. To verify this, we precisely specify the unacceptable concepts to reduce ambiguity: as *Nemo fish*, *Captain Marvel female superhero*, *Snoopy dog*, and *R2D2 robot*. We evaluate ESPRESSO on a separate validation dataset and then report the numbers for the evaluation dataset below: compared to the results

in Table 7, the normalized CLIP score for this new configuration is: 0.97 ± 0.00 (*Nemo*), 0.90 ± 0.02 (*Captain Marvel*), 0.98 ± 0.03 (*Snoopy*), 0.92 ± 0.02 (*R2D2*), which are now indicated in **green**. We also report the CLIP accuracy to evaluate effectiveness with this new configuration: 0.02 ± 0.00 (*Nemo*), 0.00 ± 0.00 (*Captain Marvel*), 0.02 ± 0.01 (*Snoopy*), 0.00 ± 0.00 (*R2D2*), which are effective, same as before. Hence, precisely specifying c^u is important for ESPRESSO and can improve utility preservation without sacrificing effectiveness. *In summary, ESPRESSO preserves utility on most concepts, and the poor utility can be improved by a careful choice of c^u .*

R3 Robustness. We report CLIP accuracy in Table 8 on \mathcal{D}_{ado}^u . We evaluate different CRTs against four attacks: Typo+, PEZ+, CCE/CCE+, and RingBell+. We evaluate fine-tuning CRT’s against CCE, and evaluate ESPRESSO against CCE+ as CCE already accounts for fine-tuning CRTs. We use the same color coding as in Table 6.

CCE/CCE+, being a white-box attack which uses the parameters of the entire T2I model, is the strongest attack and it makes all fine-tuning CRTs ineffective. However, ESPRESSO is effective against CCE/CCE+ and outperforms all fine-tuning CRTs. On the remaining attacks, all the fine-tuning CRTs have better robustness on Group-3 concepts than on Group-1 and 2. We attribute this to the difficulty of T2I models in generating precise faces while also evading detection, as shown in prior works [35]. Similar to results in Table 6, we note that all CRTs perform poorly on *nudity* and *violence* across all the attacks. This is expected as the CRTs have poor effectiveness on these concepts as seen in Table 6. Hence, adversarial prompts for these concepts are likely to easily evade them. In summary, ESPRESSO is more robust than all prior fine-tuning CRTs on all the concepts

Table 8: R3 (Robustness): Comparison with fine-tuning CRTs using CLIP accuracy on *adversarial* prompts (lower is better). We evaluate fine-tuning CRT’s against CCE and ESPRESSO against CCE+ since CCE is already adapted to fine-tuning CRT’s. We use **red if accuracy is >50; **blue** if accuracy is between 25-50; **green** if accuracy is <25.**

CRT	Concepts										
	Nudity (I2P)	Violence (I2P)	Grumpy Cat	Nemo	Captain Marvel	Snoopy	R2D2	Taylor Swift	Angelina Jolie	Brad Pitt	Elon Musk
	Typo+										
CA [27]	0.58 ± 0.02	0.75 ± 0.01	0.26 ± 0.02	0.27 ± 0.01	0.42 ± 0.01	0.29 ± 0.02	0.23 ± 0.02	0.09 ± 0.02	0.24 ± 0.01	0.05 ± 0.01	0.31 ± 0.06
FMN [64]	0.61 ± 0.02	0.75 ± 0.02	0.21 ± 0.01	0.31 ± 0.01	0.49 ± 0.02	0.27 ± 0.02	0.22 ± 0.02	0.03 ± 0.01	0.17 ± 0.01	0.06 ± 0.01	0.34 ± 0.01
SA [18]	0.31 ± 0.01	0.71 ± 0.02	0.99 ± 0.01	0.94 ± 0.01	0.89 ± 0.02	0.73 ± 0.03	0.99 ± 0.00	0.20 ± 0.02	0.05 ± 0.01	0.43 ± 0.04	0.65 ± 0.05
ESD [13]	0.39 ± 0.01	0.70 ± 0.01	0.27 ± 0.02	0.25 ± 0.05	0.40 ± 0.03	0.23 ± 0.02	0.25 ± 0.05	0.03 ± 0.01	0.08 ± 0.07	0.04 ± 0.03	0.23 ± 0.05
UCE [16]	0.41 ± 0.00	0.60 ± 0.00	0.28 ± 0.02	0.29 ± 0.02	0.34 ± 0.02	0.21 ± 0.03	0.17 ± 0.02	0.00 ± 0.00	0.05 ± 0.00	0.02 ± 0.00	0.12 ± 0.00
SDD [23]	0.20 ± 0.02	0.50 ± 0.04	0.27 ± 0.02	0.21 ± 0.02	0.48 ± 0.01	0.19 ± 0.01	0.31 ± 0.00	0.05 ± 0.01	0.06 ± 0.00	0.05 ± 0.00	0.10 ± 0.01
ESPRESSO	0.14 ± 0.01	0.20 ± 0.01	0.10 ± 0.01	0.06 ± 0.01	0.09 ± 0.01	0.09 ± 0.01	0.08 ± 0.01	0.00 ± 0.01	0.00 ± 0.01	0.01 ± 0.01	0.01 ± 0.01
	PEZ+										
CA [27]	0.75 ± 0.01	0.84 ± 0.02	0.33 ± 0.04	0.52 ± 0.01	0.70 ± 0.02	0.20 ± 0.01	0.25 ± 0.03	0.46 ± 0.01	0.64 ± 0.01	0.63 ± 0.02	0.72 ± 0.01
FMN [64]	0.74 ± 0.01	0.72 ± 0.02	0.43 ± 0.02	0.41 ± 0.01	0.85 ± 0.03	0.45 ± 0.01	0.93 ± 0.06	0.04 ± 0.01	0.16 ± 0.01	0.08 ± 0.01	0.23 ± 0.01
SA [18]	0.55 ± 0.03	0.82 ± 0.01	0.14 ± 0.00	0.14 ± 0.00	0.14 ± 0.01	0.15 ± 0.01	0.15 ± 0.00	0.15 ± 0.01	0.15 ± 0.01	0.14 ± 0.00	0.15 ± 0.01
ESD [13]	0.69 ± 0.01	0.88 ± 0.01	0.36 ± 0.06	0.40 ± 0.04	0.44 ± 0.02	0.34 ± 0.03	0.26 ± 0.03	0.05 ± 0.02	0.11 ± 0.04	0.17 ± 0.02	0.23 ± 0.03
UCE [16]	0.59 ± 0.00	0.82 ± 0.00	0.23 ± 0.01	0.52 ± 0.01	0.59 ± 0.03	0.14 ± 0.02	0.25 ± 0.02	0.00 ± 0.00	0.06 ± 0.01	0.06 ± 0.01	0.15 ± 0.02
SDD [23]	0.30 ± 0.01	0.60 ± 0.01	0.28 ± 0.05	0.28 ± 0.01	0.50 ± 0.03	0.34 ± 0.03	0.30 ± 0.03	0.04 ± 0.01	0.09 ± 0.02	0.06 ± 0.01	0.12 ± 0.01
ESPRESSO	0.15 ± 0.01	0.25 ± 0.05	0.10 ± 0.01	0.12 ± 0.01	0.11 ± 0.03	0.08 ± 0.01	0.03 ± 0.00	0.00 ± 0.01	0.03 ± 0.00	0.04 ± 0.00	0.04 ± 0.00
	RingBell+										
CA [27]	0.97 ± 0.01	0.96 ± 0.01	0.79 ± 0.01	0.76 ± 0.02	0.88 ± 0.02	0.38 ± 0.02	0.65 ± 0.05	0.03 ± 0.03	0.00 ± 0.01	0.88 ± 0.01	1.00 ± 0.01
FMN [64]	0.96 ± 0.01	0.95 ± 0.02	0.75 ± 0.00	0.57 ± 0.01	0.91 ± 0.00	0.45 ± 0.01	0.59 ± 0.01	0.26 ± 0.01	0.85 ± 0.02	0.88 ± 0.01	0.99 ± 0.02
SA [18]	0.80 ± 0.02	0.98 ± 0.02	0.93 ± 0.02	0.98 ± 0.01	0.96 ± 0.03	0.97 ± 0.03	0.88 ± 0.02	0.00 ± 0.01	0.03 ± 0.02	0.77 ± 0.10	1.00 ± 0.01
ESD [13]	0.77 ± 0.03	0.95 ± 0.02	0.63 ± 0.06	0.66 ± 0.12	0.56 ± 0.06	0.66 ± 0.07	0.69 ± 0.01	0.00 ± 0.00	0.03 ± 0.02	0.27 ± 0.03	0.55 ± 0.08
UCE [16]	0.84 ± 0.00	0.67 ± 0.00	0.38 ± 0.05	0.74 ± 0.01	0.07 ± 0.00	0.16 ± 0.01	0.50 ± 0.01	0.05 ± 0.00	0.01 ± 0.00	0.02 ± 0.01	0.34 ± 0.01
SDD [23]	0.33 ± 0.02	0.60 ± 0.03	0.22 ± 0.01	0.31 ± 0.01	0.62 ± 0.01	0.42 ± 0.03	0.41 ± 0.01	0.07 ± 0.02	0.07 ± 0.02	0.07 ± 0.01	0.17 ± 0.02
ESPRESSO	0.05 ± 0.01	0.08 ± 0.01	0.20 ± 0.08	0.15 ± 0.03	0.04 ± 0.02	0.01 ± 0.01	0.15 ± 0.05	0.00 ± 0.02	0.03 ± 0.02	0.01 ± 0.02	0.02 ± 0.02
	CCE or CCE+ (against ESPRESSO)										
CA [27]	1.00 ± 0.00	1.00 ± 0.00	1.00 ± 0.00	0.99 ± 0.00	0.97 ± 0.01	1.00 ± 0.00	0.99 ± 0.01	1.00 ± 0.00	1.00 ± 0.00	1.00 ± 0.00	0.80 ± 0.00
FMN [64]	1.00 ± 0.00	1.00 ± 0.00	0.99 ± 0.00	0.99 ± 0.00	0.98 ± 0.00	0.98 ± 0.01	0.99 ± 0.00	0.99 ± 0.00	1.00 ± 0.00	0.99 ± 0.00	0.99 ± 0.00
SA [18]	0.98 ± 0.01	0.99 ± 0.01	0.99 ± 0.00	0.97 ± 0.01	1.00 ± 0.00	0.99 ± 0.00	0.99 ± 0.00	1.00 ± 0.00	0.84 ± 0.01	0.97 ± 0.00	0.81 ± 0.01
ESD [13]	0.92 ± 0.00	0.99 ± 0.00	0.91 ± 0.01	0.94 ± 0.00	0.96 ± 0.00	0.99 ± 0.00	0.99 ± 0.00	1.00 ± 0.00	1.00 ± 0.00	1.00 ± 0.00	0.98 ± 0.01
UCE [16]	1.00 ± 0.00	0.97 ± 0.00	1.00 ± 0.00	0.98 ± 0.00	0.98 ± 0.01	1.00 ± 0.00	0.99 ± 0.00	0.99 ± 0.00	0.63 ± 0.01	1.00 ± 0.00	0.77 ± 0.01
SDD [23]	1.00 ± 0.00	0.81 ± 0.00	0.81 ± 0.00	0.93 ± 0.01	0.96 ± 0.00	0.98 ± 0.00	0.97 ± 0.01	0.67 ± 0.01	0.77 ± 0.01	1.00 ± 0.00	0.81 ± 0.01
ESPRESSO	0.00 ± 0.00	0.40 ± 0.05	0.02 ± 0.00	0.00 ± 0.00	0.00 ± 0.00	0.00 ± 0.01	0.00 ± 0.00	0.00 ± 0.00	0.00 ± 0.00	0.00 ± 0.00	0.01 ± 0.01

across all the attacks. We discuss the possibility of future attacks against ESPRESSO in Section 9.2.

Summary. We depict the trade-offs among R1, R2, and R3 in Figure 1. We use (1-CLIP accuracy) for R1 on \mathcal{D}_{te}^u , normalized CLIP score on \mathcal{D}_{te}^a for R2, and (1-CLIP accuracy) for R3 on \mathcal{D}_{adv}^u using CCE/CCE+. For each of the requirements, we use the average across all concepts as the representative value for a CRT. Overall, ESPRESSO provides a better trade-off across the three requirements compared to all the other CRTs.

6.2 Comparison with Filtering CRT

We compare with UD [42], the state-of-the-art filtering CRT, across the three requirements and summarize the results. We use FNR to evaluate effectiveness on \mathcal{D}_{te}^u , FPR for utility on \mathcal{D}_{te}^a , and FNR for robustness on \mathcal{D}_{adv}^u .

R1 Effectiveness. We report FNR across four concepts (*nudity*, *violence*, *disturbing*, and *hateful*). ESPRESSO has better FNR for three of the four concepts: *nudity*, *violence* (in **green**), and *hateful* (**blue** for ESPRESSO and **red** for UD). However, both ESPRESSO and UD perform poorly on *disturbing*. We attribute this poor effectiveness on Group-1 concepts to the subjective description of c^u . Images for

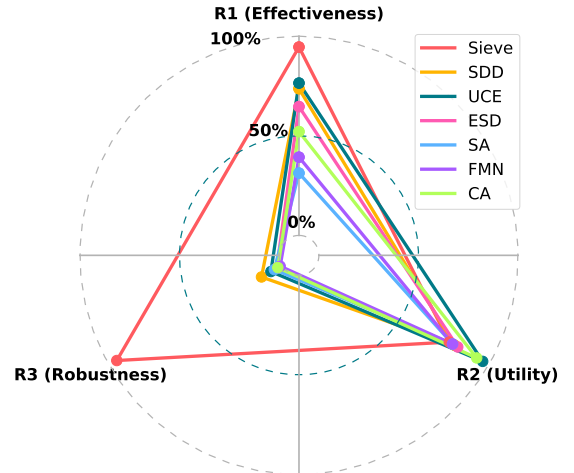


Figure 1: ESPRESSO has a better trade-off across R1, R2, and R3 compared to other fine-tuning CRTs.

these concepts cover a wide variety of sub-concepts simultaneously which are not precisely identified for CRTs.

Table 9: R1 (Effectiveness): Comparison with filtering CRT (UD) using FNR on *unacceptable* prompts (lower is better). We use **red if FNR is >0.50 ; **blue** if FNR is between $0.25-0.50$; **green** if FNR is <0.25 .**

Concepts	UD	ESPRESSO
Nudity (I2P)	0.39 ± 0.02	0.14 ± 0.05
Violence (I2P)	0.90 ± 0.02	0.20 ± 0.00
Disturbing (I2P)	0.89 ± 0.03	0.53 ± 0.08
Hateful (I2P)	1.00 ± 0.00	0.42 ± 0.03

Table 10: R2 (Utility): Comparison with filtering CRT (UD) using FPR on *acceptable* prompts (lower is better). We use **red if FPR is >0.50 , **blue** if FPR is between $0.25-0.50$; **green** if FPR is <0.25 .**

Concepts	UD	ESPRESSO
Nudity (I2P)	0.01 ± 0.00	0.01 ± 0.01
Violence (I2P)	0.01 ± 0.00	0.08 ± 0.05
Disturbing (I2P)	0.01 ± 0.00	0.01 ± 0.01
Hateful (I2P)	0.01 ± 0.00	0.06 ± 0.04

R2 Utility. We present FPR in Table 10 across the four Group-1 concepts. As expected, we observe that both ESPRESSO and UD perform well since they demonstrate a low FPR. This is expected since UD explicitly includes images containing c^a while training the multi-headed classifier.

R3 Robustness. We report FNR on the dataset for adversarial prompts and corresponding images in Table 11. In addition to the four attacks from Table 8, recall that SneakyPrompt [63] is specifically designed to attack filtering CRTs. Hence, we also include the evaluation against SneakyPrompt. Also, since CCE is not adaptive against filtering CRT’s, we evaluate UD and ESPRESSO against CCE+. We are the first to show the effectiveness of different attacks against UD.

Table 11: R3 (Robustness): Comparison with filtering CRT (UD) using FNR on *adversarial* prompts (lower is better). We use **red if FNR is >0.50 ; **blue** if FNR is between $0.25-0.50$; and **green** if FNR is <0.25 .**

CRT	Nudity	Violence	Disturbing	Hateful
	Typo+			
UD	0.55 ± 0.02	0.91 ± 0.05	0.39 ± 0.01	0.48 ± 0.01
ESPRESSO	0.15 ± 0.01	0.26 ± 0.01	0.39 ± 0.01	0.37 ± 0.05
	PEZ+			
UD	0.65 ± 0.02	0.91 ± 0.02	0.89 ± 0.02	1.00 ± 0.00
ESPRESSO	0.16 ± 0.02	0.25 ± 0.04	0.14 ± 0.03	0.20 ± 0.05
	CCE+			
UD	0.00 ± 0.00	0.75 ± 0.05	1.00 ± 0.05	1.00 ± 0.00
ESPRESSO	0.00 ± 0.00	0.38 ± 0.05	0.02 ± 0.01	0.02 ± 0.01
	RingBell+			
UD	0.95 ± 0.03	0.50 ± 0.04	0.30 ± 0.05	0.90 ± 0.05
ESPRESSO	0.06 ± 0.08	0.08 ± 0.01	0.06 ± 0.02	0.25 ± 0.05
	SneakyPrompt			
UD	0.67 ± 0.21	0.71 ± 0.02	0.82 ± 0.03	0.48 ± 0.06
ESPRESSO	0.40 ± 0.08	0.14 ± 0.03	0.70 ± 0.05	0.15 ± 0.10

We observe that ESPRESSO is effective in thwarting p^{adv} s from PEZ+ while UD can be evaded. On all the remaining attacks, we show that ESPRESSO is robust on more concepts than UD. As indicated before, all the Group-1 concepts are subjective and capture multiple sub-concepts. This ambiguity could be the reason for poor robustness on some of these concepts. Overall, ESPRESSO shows better robustness than UD on the majority of the concepts across different attacks.

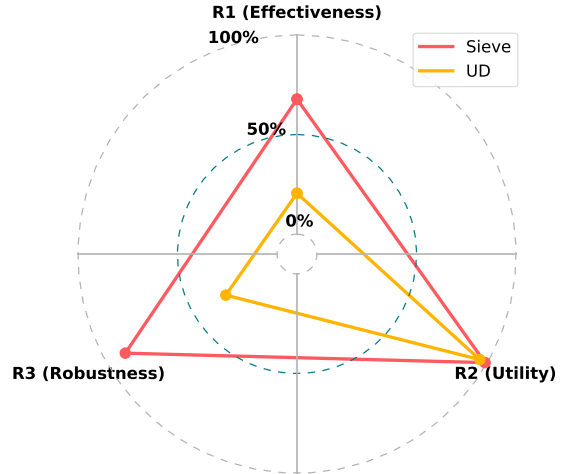


Figure 2: ESPRESSO has a better trade-off across R1, R2, and R3 compared to filtering CRT (UD).

Summary. We present the trade-offs in the form of radar plots in Figure 2. We use $(1 - \text{FNR})$ on \mathcal{D}_{te}^u for **R1**, $(1 - \text{FPR})$ on \mathcal{D}_{te}^a for **R2**, and $(1 - \text{FNR})$ on \mathcal{D}_{adv}^u using CCE+ for **R3**. Hence, a higher value indicates better performance. ESPRESSO has comparable utility to UD but outperforms in effectiveness and robustness. Overall, ESPRESSO covers a larger area, and hence provides a better trade-off compared to UD.

7 CERTIFYING ROBUSTNESS OF ESPRESSO

We showed empirically that ESPRESSO is robust against several state-of-the-art attacks (Section 6). Inspired by the literature on certified robustness against adversarial examples [9], it is natural to ask whether a similar notion of certified robustness is possible for CRTs. None of the existing CRTs have considered certified robustness. To this end, we are the first to explore its feasibility for ESPRESSO.

We first present a theoretical bound on the worst-case modification by \mathcal{A}_{adv} under which we can guarantee ESPRESSO’s accuracy (Section 7.1). We then empirically evaluate this bound on different concepts (Section 7.2) and finally discuss some implications of our results (Section 7.3).

7.1 Theoretical Bound

Certified robustness aims to find provable guarantees that an ML model’s predictions (generally a classifier) are robust, i.e., the predictions do not change on adding noise to the input [6]. Our goal is to have a similar provable robustness bound for a T2I model with

ESPRESSO. We want to find the maximum noise to an input which ESPRESSO can tolerate.

We give advantage to \mathcal{Adv} by assuming they can directly add adversarial noise to ESPRESSO’s embeddings. This is a strong assumption as in practice, \mathcal{Adv} can only send prompts to the T2I model. We revisit this assumption later in Section 7.3. Formally, given an unacceptable image x^u , \mathcal{Adv} adds noise δ to its embeddings, $\phi_x(x^u)$, such that $F(\phi_x(x^u) + \delta)$ is misclassified as acceptable. Using this assumption, we specify the maximum noise δ added to the embeddings, $\phi_x(x^u)$, that ESPRESSO can tolerate in Theorem 7.1.

THEOREM 7.1. *Let $\hat{x} = \phi_x(x)$, $\hat{c}^i = \phi_p(c^i)$, $i \in \{a, u\}$. Define*

$$g_i(\hat{x}) := \frac{\exp(s(\hat{x}, \hat{c}^i))}{\exp(s(\hat{x}, \hat{c}^a)) + \exp(s(\hat{x}, \hat{c}^u))},$$

where $s(\hat{x}, \hat{c}^i) = \tau \cos(\hat{x}, \hat{c}^i)$, then g_i is the confidence of \hat{x} being classified as c^i . $F(x)$ in equation 1 can be defined as $F(\hat{x}) = \operatorname{argmax}_i g_i(\hat{x})$, and $F(\hat{x})$ classifies \hat{x} as unacceptable if $g_u(\hat{x}) > \Gamma$, where Γ is the decision threshold. For a given image embedding \hat{x} , if $g(\hat{x}) := g_u(\hat{x}) > \Gamma$, then g is robust against noise δ where

$$\|\delta\| \leq \left(1 - \frac{\tau}{\tau + 2|g(\hat{x}) - \Gamma|}\right) \|\hat{x}\|,$$

and Γ is the decision threshold i.e.

$$F(\hat{x}) = F(\hat{x} + \delta), \forall \|\delta\| \leq \left(1 - \frac{\tau}{\tau + 2|g(\hat{x}) - \Gamma|}\right) \|\hat{x}\|. \quad (5)$$

Proof Sketch. We prove the above theorem by applying Lipschitz continuity over $g(\hat{x})$. $F(\cdot)$ is the composition of the softmax function and the scaled cosine similarity over the embeddings, where both functions are Lipschitz continuous when $\|\hat{x}\| > 0$. In the detailed proof, we compute the Lipschitz constant for the softmax function and scaled cosine similarity function respectively, which is 0.25 and $\frac{\tau}{\|\hat{x}\|}$. Then the Lipschitz constant for $g(\hat{x})$ will be $\frac{\tau}{2\|\hat{x}\|}$ according to the chain rule. Finally, using the triangle inequality on $|g(\hat{x}) - g(\hat{x} + \delta)|$, and plugging the bound in to the inequality, we get $g(\hat{x} + \delta) \geq \Gamma$.

PROOF. For an unacceptable image embedding $\hat{x} = \phi_x(x^u)$, $g(\hat{x}) := g_u(\hat{x})$, then $g(\hat{x}) - \Gamma > 0$, and Γ is the decision threshold for classification. Let $s_1 = \tau \cos(\hat{x}, \hat{c}^u)$, $s_2 = \tau \cos(\hat{x}, \hat{c}^a)$, $\mathbf{s} = [s_1, s_2]^T$, then

$$g(\hat{x}) = S(s_1) = \frac{\exp(s_1)}{\exp(s_1) + \exp(s_2)},$$

where $S(s_1)$ is the first item of Softmax function with respect to \mathbf{s} . Then, we have $\frac{\partial}{\partial s_1} S = S(s_1)(1 - S(s_1)) \leq 0.25$, $\frac{\partial}{\partial s_2} S = -S(s_1)S(s_2) \leq 0.25$.

Note that $\|\hat{x}\| > 0$ and $\|\hat{c}^a\| > 0$, we have

$$\begin{aligned} \left\| \frac{\partial}{\partial \hat{x}} s(\hat{x}, \hat{c}^a) \right\| &= \left\| \frac{\tau \|\hat{c}^a\| (I - \hat{x} \hat{x}^T) \hat{c}^a}{\|\hat{x}\| \|\hat{c}^a\|^2} \right\| \\ &= \frac{\tau \sin(\hat{x}, \hat{c}^a)}{\|\hat{x}\|} \leq \frac{\tau}{\|\hat{x}\|}. \end{aligned}$$

And $\left\| \frac{\partial}{\partial \hat{x}} s(\hat{x}, \hat{c}^u) \right\| \leq \frac{\tau}{\|\hat{x}\|}$.

For each \hat{x} , according to the chain rule of composition functions, $\frac{\partial}{\partial \hat{x}} g(\hat{x}) = \frac{\partial S}{\partial s_1} \cdot \frac{\partial s_1}{\partial \hat{x}} + \frac{\partial S}{\partial s_2} \cdot \frac{\partial s_2}{\partial \hat{x}} \leq \frac{\tau}{2\|\hat{x}\|}$. Therefore the Lipschitz

constant of $g(\hat{x})$ with respect to \hat{x} is $\frac{\tau}{2\|\hat{x}\|}$, and

$$\begin{aligned} \|g(\hat{x} + \delta) - g(\hat{x})\| &\leq \frac{1}{2} \frac{\tau}{\min\{\|\hat{x}\|, \|\delta\|\}} \|\delta\| \\ &\leq \frac{1}{2} \frac{\tau}{\|\hat{x}\| - \|\delta\|} \|\delta\|, \end{aligned}$$

where $U(\hat{x}, \delta)$ is a l_2 -ball of \hat{x} with radius δ .

When $\|\delta\| \leq (1 - \frac{\tau}{\tau + 2|g(\hat{x}) - \Gamma|}) \|\hat{x}\| < \|\hat{x}\|$, we have

$$\begin{aligned} |g(\hat{x} + \delta) - g(\hat{x})| &= \|g(\hat{x} + \delta) - g(\hat{x})\| \\ &\leq \frac{\tau}{2 \left(\frac{\|\hat{x}\|}{\|\delta\|} - 1 \right)} \\ &\leq \frac{\tau}{2 \left(\frac{\tau + 2|g(\hat{x}) - \Gamma|}{2|g(\hat{x}) - \Gamma|} - 1 \right)} \\ &\leq |g(\hat{x}) - \Gamma| = g(\hat{x}) - \Gamma. \end{aligned}$$

Then,

$$\begin{aligned} g(\hat{x} + \delta) &\geq |g(\hat{x})| - |g(\hat{x} + \delta) - g(\hat{x})| \\ &\geq g(\hat{x}) - |g(\hat{x}) - \Gamma| \geq \Gamma, \end{aligned} \quad (6)$$

which concludes the proof. \square

7.2 Empirical Validation

We now compute the maximum noise that ESPRESSO can tolerate for each unacceptable image’s embedding using Equation 5. Following prior literature on certified robustness [9], we compute the certified accuracy described in [9] to evaluate the robustness of ESPRESSO. Certified accuracy at radius r is the fraction of unacceptable images which are correctly classified and are robust against adversarial noise $\delta > r$. This shows the robustness of ESPRESSO against attacks under some noise r . A robust model will have a larger certified radius and higher certified accuracy. Since we add noise directly to $\phi_x(x^u)$, we compare our certified accuracy with the accuracy of clean unacceptable images (without adversarial noise) which we refer as “clean accuracy”. Ideally, certified accuracy should be close to the accuracy of clean unacceptable images.

We present the results in Figure 3 for the three groups of concepts. Clean accuracy in Figure 3 is the certified accuracy at radius zero. ESPRESSO is robust against $\delta < 0.07$, incurring less than a 5% drop in certified accuracy. When $\delta < 0.15$, the certified accuracy remains higher than 50% for all concepts. ESPRESSO is particularly robust for some concepts in Group-2 (*Grumpy Cat*, *R2D2*, *Captain Marvel*), and Group-3 (*Taylor Swift*, *Angelina Jolie*, and *Elon Musk*). For these concepts, the certified accuracy remains the same for the clean unacceptable images until $\delta > 0.15$. Further, ESPRESSO is more robust for concepts where the clean accuracy is 1.00 (CLIP accuracy from Table 6). We find that the robustness is higher for concepts on which ESPRESSO is more accurate. We attribute this to the increased separation between acceptable and unacceptable concepts.

7.3 Practical Implications

Having discussed the theoretical bound and empirically validated it on different concepts, we now revisit the practicality of this bound. We first discuss the usefulness of the certification followed by our assumption about \mathcal{Adv} ’s capability.

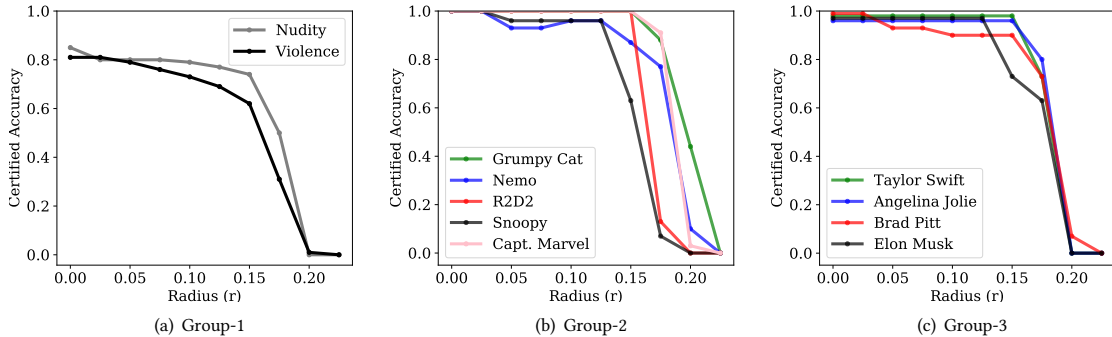


Figure 3: Certified accuracy of ESPRESSO vs. adversarial noise δ , for a strong $\mathcal{A}dv$ with access to embeddings of generated images.

Usefulness of Certified Bound. In Figure 3, we find that the certified bound is less than 0.15 across all the concepts. We found this to be smaller than the l_2 -norms of realistic image embeddings, which had a mean of 17. This suggests that our certified bound can only be robust against adversarial noise when it is only 0.8% ($=0.15/17$) of the embeddings.

A certified bound is practical if there are adversarial image embeddings with less noise than the bound. Then, the bound is effective against these embeddings. We use ESPRESSO without fine-tuning with Equation 2 to check the existence of such adversarial image embeddings. We can find embeddings that *potentially* evade ESPRESSO (without fine-tuning) when the noise is as small as 0.028. Our certified bound is useful against such embeddings².

However, the distance between acceptable and unacceptable images, which is at least 7, is much larger than the certified bound. This suggests that our certified bound is loose. We leave a tighter certified bound and the possibility of using adversarial training for improving robustness as future work (c.f. Section 9.2).

$\mathcal{A}dv$'s Capability. To compute the certified bound, we assumed a strong $\mathcal{A}dv$ who can directly add adversarial noise to the *embeddings*. In practice, $\mathcal{A}dv$ can only modify the *prompts* sent to the T2I model, and can only obtain the corresponding filtered outputs. Hence, in practice, $\mathcal{A}dv$ is much weaker and the robustness of ESPRESSO is much higher than indicated in Figure 3.

To illustrate this, we consider a concrete attack approach that $\mathcal{A}dv$ could adopt given its inability to directly add adversarial noise to embeddings: $\mathcal{A}dv$ can begin with unacceptable images and incorporate adversarial noise using standard evasion techniques (e.g., PGD [34]) to find an adversarial example that evades the ESPRESSO classifier. $\mathcal{A}dv$ can then find the corresponding adversarial prompt using one of the attacks (PEZ+) in Section 2.3. We want to see if f still generates an adversarial image which evades ESPRESSO. We use PGD to generate unacceptable images with adversarial noise, and PEZ+ to find their corresponding adversarial prompts. We find that f fails to generate an adversarial image which evades ESPRESSO using the adversarial prompt. This is due to the adversarial-prompt-generation process being an approximation, which fails to fully

²Note that to find an actual attack against ESPRESSO, $\mathcal{A}dv$ will have to (a) find a prompt that generates this perturbed embedding, and (b) ensure that the resulting image retains the unacceptable content.

capture all aspects of the adversarial image. Moreover, using the T2I model to generate the image from the adversarial prompt is unlikely to capture the adversarial noise due to the de-noising used in the diffusion model (Section 2.1). This claim is further supported by prior literature on the robustness of diffusion models [7, 22, 60, 66].

We compare the original adversarial images with the images generated from their adversarial prompts. We present one concept from each group in Appendix A: Figure 4. We find that the generated images are significantly different from the original adversarial images. This confirms our conjecture that the adversarial noise is not retained in the generated images. A more thorough exploration of such an attack is left as future work. Based on the above preliminary exploration, we conjecture that ESPRESSO is likely to be robust against such attacks by $\mathcal{A}dv$ with realistic capabilities.

8 RELATED WORK

Prompt Filters. We focus on image filters to detect x^u . Prior works have explored using prompt filters to identify unacceptable concepts before passing them to T2I models [62]. Such filters are being used for DALLE-2 [44], and MidJourney [36]. However, these prompt filters are not robust and easy to evade [1, 33]. Hence, prior works have identified image filters are a better alternative, with the possibility of making it effective and robust [30].

Additional CRTs. We use state-of-the-art CRTs for evaluation. Hence, we omit the discussion about prior CRTs which have been outperformed by those considered in this work [40, 43, 49]. We discuss some recent fine-tuning CRTs.

Hong et al. [20] propose an approach to make minimal changes for concept removal. Instead of matching the entire distribution of features for c^u to the distribution of c^a , they selectively modify the features with highest density in c^u . Wu et al. [58] propose concept removal as an unlearning problem which is solved as constraint optimization while preserving utility. Basu et al. [2] present a closed-form solution to remove concepts from ϕ by identifying causal features for one concept and overriding it with another concept. Since these approaches are similar to other fine-tuning CRTs considered in this work, and do not optimize for robustness, we conjecture that these approaches are susceptible to evasion.

Huang et al. [21] modify the cross entropy layers of ϵ_θ to erase c^u with adversarial training for better robustness against only two

naïve attacks: Prompting4Debugging [8] and RingBell [53]. Li et al. [30] modify the self-attention layers of ϵ_θ using triplets of x^u , censored x^u , and x^a . They evaluate robustness against SneakyPrompt. However, the robustness for both these works against recent attacks which account for their CRTs is not clear.

Pham et al. [39] fine-tune T2I model to generate a specific concept and subtract the task vector for this concept from the model parameters of the original model, thereby erasing c^u . They demonstrate robustness against CCE and RingBell but suffers from a trade-off between **R2** and **R3**. Wu et al. [59] insert backdoors to textual inversion embeddings such that a c^u results in a pre-defined image instead of x^u . Despite accounting for robustness, these CRTs incur trade-offs between **R1**, **R2**, and **R3**, inherent to fine-tuning CRTs.

Additional Attacks against CRTs. Prompting4Debugging uses PEZ while matching the noise between a T2I model with a CRT, and one without a CRT, during the reverse diffusion process. In our setting, T2I model with and without ESPRESSO are identical, hence Prompting4Debugging reduces to PEZ. Rando et al. [45] propose PromptDilution against filters. However, as SneakyPrompt outperformed PromptDilution [63], we do not consider it for evaluation.

Ba et al. [1] generate substitutes for c^u in their input prompts to evade a black-box filter. They show effectiveness against the Q16 filter which is outperformed by UD. Ma et al. [33] optimize for p^{adv} such that it matches c^u using TextGrad, a gradient based search over text, to identify the tokens. Their attack outperforms Prompting4Debugging, Prompt Dilution, and RingBell. Shahgir [51] replace an object in x with another targeted object to create x^{adv} , which can be inverted to get p^{adv} . Kou et al. [26] use a character-level gradient attack that replaces specific characters for p^{adv} .

9 DISCUSSION AND FUTURE WORK

We discuss efficiency of CRTs (Section 9.1), accounting for future attacks (Section 9.2), applicability/extensions of ESPRESSO (Section 9.3), and a summary of this work (Section 9.4).

9.1 Efficiency of CRTs

In Table 12, we report the execution time for fine-tuning or training the CRTs (average across ten runs). For related work, the configuration for fine-tuning/training is the same as specified by their respective paper to satisfy **R1** and **R2**. These times were obtained from training on a single NVIDIA A100 GPU.

Table 12: Efficiency: CRT training time (mean across ten runs).

Technique	Time (mins)	Technique	Time (mins)
CA [27]	60.03 ± 0.01	UCE [16]	0.24 ± 0.02
SA [18]	95.10 ± 2.21	ESD [13]	125.50 ± 0.00
SDD [23]	75.50 ± 3.21	UD [42]	10.00 ± 2.03
FMN [64]	2.20 ± 0.01	ESPRESSO	9.10 ± 0.05

ESPRESSO is reasonably fast to train. For fine-tuning CRTs inference time is identical to using the baseline SD v1.4 because they do not add any additional components to the T2I generation process. The inference time for filtering CRTs is marginally higher (+0.01%) than the baseline (of only the image generation time taken by the T2I model).

9.2 Addressing Future Attacks

Recall that our certified robustness bound is loose (Section 7). We leave the improvement of the bound as future work.

ESPRESSO maintains high robustness across all evaluated concepts. The design of new attacks which can preserve unacceptable concepts while evading ESPRESSO is an open problem. Adversarial training for ESPRESSO can be used to increase its robustness.

We can fine-tune CLIP with this objective: $\mathcal{L}_{\text{Con-adv}}(\mathcal{D}_{adv}^u) =$

$$-\frac{1}{N} \sum_{j=1}^N \log \frac{\exp(\cos(\phi_x(x_j^{adv}), \phi_p(c^u))/\tau)}{\sum_{k \in \{a,u\}} \exp(\cos(\phi_x(x_j^{adv}), \phi_p(c_k))/\tau)}$$

where $\mathcal{D}_{adv} = \{(x_j^{adv}, p_j^{adv})\}_{j=1}^N$. Assuming x^{adv} evades the filter, we optimize ϕ_p and ϕ_x , such that $\phi_p(x_j^{adv})$ is closer to $\phi_p(c^u)$ than $\phi_p(c^a)$. This loss would be added to Equation 2 and 3. Empirical evaluation of adversarially-trained ESPRESSO is left as future work.

9.3 Applications and Extensions to ESPRESSO

Filtering Multiple Concepts. Gandikota et al. [16] have considered removing multiple concepts simultaneously. While we focus on filtering one concept at a time for comparison with other CRTs, ESPRESSO can be extended by including multiple concepts simultaneously as well. Specifically, for $F(x, c^u, c^a)$ in Equation 1, instead of only specifying c^u and c^a for a single concept, we can include c^u and c^a for multiple concepts as a list. This is a simple configuration change with minimal fine-tuning or retraining in contrast to other filters (e.g., [42]) which require training with extensive datasets. We leave the evaluation of different requirements on filtering multiple concepts in ESPRESSO as future work.

Filtering Artistic Styles. None of the prior filtering CRTs consider any copyrighted content and focus on only *inappropriate Group-1 concepts*. ESPRESSO is the first filtering CRT which is applicable to concepts which are copyright-infringing (Group-2) or involve unauthorized use of personalized images (Group-3). Prior fine-tuning CRTs have considered removing artistic styles (e.g., painting in the style of Monet or Van Gogh) as copyrighted content [13, 27]. However, we observed that ESPRESSO does not differentiate between images with and without artistic styles very well. Specifically, *Monet painting as c^u* and *painting as c^a* , are very similar for ESPRESSO, thus reducing its effectiveness. We leave the optimization of ESPRESSO to account for artistic styles as future work.

Applicability to other T2I Models. Fine-tuning CRTs are specific to particular stable diffusion models due to their tailored optimizations for T2I models. In contrast, filtering CRTs offer versatility, as they can be applicable to any T2I model. Filters analyze only the generated image and the list of concepts, independently of the T2I model. However, fine-tuning the filter using data from T2I model, as we do it for ESPRESSO, can improve effectiveness and utility. This allows to use the filter we will have a filter that will work with T2I model in different domains (e.g., anime images). Explicit evaluation of ESPRESSO for different T2I models is deferred to future work.

9.4 Summary

Removing unacceptable concepts from T2I models is an important problem. However, none of the prior CRTs satisfy all three

requirements simultaneously: effectiveness in removing unacceptable concepts, preserve utility on other concepts, and robustness against evasion. We propose ESPRESSO, the *first robust filtering* CRT which meets all the three requirements simultaneously and achieves a better trade-off than prior CRTs.

ACKNOWLEDGMENTS

This work is supported in part by Intel (in the context of Private AI consortium), and the Government of Ontario. Views expressed in the paper are those of the authors and do not necessarily reflect the position of the funding agencies.

REFERENCES

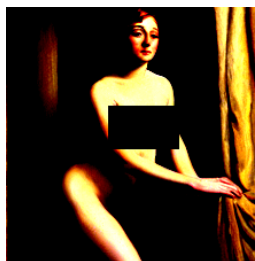
- [1] Zhongjie Ba, Jieming Zhong, Jiachen Lei, Peng Cheng, Qinglong Wang, Zhan Qin, Zhibo Wang, and Kui Ren. 2023. SurrogatePrompt: Bypassing the Safety Filter of Text-To-Image Models via Substitution. arXiv:2309.14122 [cs.CV]
- [2] Samyadeep Basu, Nanxuan Zhao, Vlad I Morariu, Soheil Feizi, and Varun Manjunatha. 2024. Localizing and Editing Knowledge In Text-to-Image Generative Models. In *The Twelfth International Conference on Learning Representations*. OpenReview.net. <https://openreview.net/forum?id=Qmw9ne6SOQ>
- [3] Arjun Nitin Bhagoji, Daniel Cullina, Chawin Sitawarin, and Prateek Mittal. 2018. Enhancing robustness of machine learning systems via data transformations. In *2018 52nd Annual Conference on Information Sciences and Systems (CISS)*. 1–5. <https://doi.org/10.1109/CISS.2018.8362326>
- [4] Nicholas Carlini, Jamie Hayes, Milad Nasr, Matthew Jagielski, Vikash Swagat, Florian Tramèr, Borja Balle, Daphne Ippolito, and Eric Wallace. 2023. Extracting training data from diffusion models. In *Proceedings of the 32nd USENIX Conference on Security Symposium (Anaheim, CA, USA) (SEC '23)*. USENIX Association, USA, Article 294, 18 pages.
- [5] Nicholas Carlini and Andreas Terzis. 2022. Poisoning and Backdooring Contrastive Learning. In *International Conference on Learning Representations*. <https://openreview.net/forum?id=iC4UHbQ01Mp>
- [6] Nicholas Carlini, Florian Tramèr, Krishnamurthy Dj Dvijotham, Leslie Rice, Mingjie Sun, and J Zico Kolter. 2023. (Certified!) Adversarial Robustness for Free!. In *The Eleventh International Conference on Learning Representations*. <https://openreview.net/forum?id=JLg5aHHv7j>
- [7] Huanran Chen, Yinpeng Dong, Shitong Shao, Zhongkai Hao, Xiao Yang, Hang Su, and Jun Zhu. 2024. Your Diffusion Model is Secretly a Certifiably Robust Classifier. arXiv:2402.02316 [cs.LG]
- [8] Zhi-Yi Chin, Chieh-Ming Jiang, Ching-Chun Huang, Pin-Yu Chen, and Wei-Chen Chiu. 2023. Prompting4Debugging: Red-Teaming Text-to-Image Diffusion Models by Finding Problematic Prompts.
- [9] Jeremy Cohen, Elan Rosenfeld, and Zico Kolter. 2019. Certified Adversarial Robustness via Randomized Smoothing. In *Proceedings of the 36th International Conference on Machine Learning (Proceedings of Machine Learning Research, Vol. 97)*, Kamalika Chaudhuri and Ruslan Salakhutdinov (Eds.). PMLR, 1310–1320. <https://proceedings.mlr.press/v97/cohen19c.html>
- [10] Will Friedwald. 2019. Captain Marvel vs. captain Marvel: The strange tale of two dueling superheroes. <https://www.vanityfair.com/hollywood/2019/03/captain-marvel-shazam-carol-danvers-guide>
- [11] Rinon Gal, Yuval Alaluf, Yuval Atzmon, Or Patashnik, Amit Haim Bermano, Gal Chechik, and Daniel Cohen-or. 2023. An Image is Worth One Word: Personalizing Text-to-Image Generation using Textual Inversion. In *The Eleventh International Conference on Learning Representations*. <https://openreview.net/forum?id=NAQvF08TcyG>
- [12] Rinon Gal, Or Patashnik, Haggai Maron, Amit H. Bermano, Gal Chechik, and Daniel Cohen-Or. 2022. StyleGAN-NADA: CLIP-guided domain adaptation of image generators. *ACM Trans. Graph.* 41, 4, Article 141, 13 pages. <https://doi.org/10.1145/3528223.3530164>
- [13] Rohit Gandikota, Joanna Materzyńska, Jaden Fiotto-Kaufman, and David Bau. 2023. Erasing Concepts from Diffusion Models. In *Proceedings of the IEEE/CVF International Conference on Computer Vision (ICCV)*. 2426–2436.
- [14] Rohit Gandikota, Joanna Materzyńska, Jaden Fiotto-Kaufman, and David Bau. 2023. GitHub - rohitgandikota/erasing: Erasing Concepts from Diffusion Models — github.com. <https://github.com/rohitgandikota/erasing>.
- [15] Rohit Gandikota, Hadas Orgad, Yonatan Belinkov, Joanna Materzyńska, and David Bau. 2023. GitHub - rohitgandikota/unified-concept-editing: Unified Concept Editing in Diffusion Models — github.com. <https://github.com/rohitgandikota/unified-concept-editing/tree/main>.
- [16] Rohit Gandikota, Hadas Orgad, Yonatan Belinkov, Joanna Materzyńska, and David Bau. 2024. Unified Concept Editing in Diffusion Models. In *Proceedings of the IEEE/CVF Winter Conference on Applications of Computer Vision (WACV)*. 5111–5120.
- [17] Alvin Heng and Harold Soh. 2023. GitHub - clear-nus/selective-amnesia — github.com. <https://github.com/clear-nus/selective-amnesia/tree/main>.
- [18] Alvin Heng and Harold Soh. 2023. Selective Amnesia: A Continual Learning Approach to Forgetting in Deep Generative Models. In *Thirty-seventh Conference on Neural Information Processing Systems*. <https://openreview.net/forum?id=BC1JdsuYB>
- [19] Jack Hessel, Ari Holtzman, Maxwell Forbes, Ronan Le Bras, and Yejin Choi. 2021. CLIPScore: A Reference-free Evaluation Metric for Image Captioning. In *Proceedings of the 2021 Conference on Empirical Methods in Natural Language Processing*, Marie-Francine Moens, Xuanjing Huang, Lucia Specia, and Scott Wen-tau Yih (Eds.). Association for Computational Linguistics, Online and Punta Cana, Dominican Republic, 7514–7528. <https://doi.org/10.18653/v1/2021.emnlp-main.595>
- [20] Seunghoo Hong, Juhun Lee, and Simon S. Woo. 2023. All but One: Surgical Concept Erasing with Model Preservation in Text-to-Image Diffusion Models. arXiv:2312.12807 [cs.CV]
- [21] Chi-Pin Huang, Kai-Po Chang, Chung-Ting Tsai, Yung-Hsuan Lai, Fu-En Yang, and Yu-Chiang Frank Wang. 2024. Receler: Reliable Concept Erasing of Text-to-Image Diffusion Models via Lightweight Erasers. arXiv:2311.17717 [cs.CV]
- [22] Gwanghyun Kim, Taesung Kwon, and Jong Chul Ye. 2022. DiffusionCLIP: Text-Guided Diffusion Models for Robust Image Manipulation. In *Proceedings of the IEEE/CVF Conference on Computer Vision and Pattern Recognition (CVPR)*. 2426–2435.
- [23] Sanghyun Kim, Seohyeon Jung, Balhae Kim, Moonseok Choi, Jinwoo Shin, and Juho Lee. 2023. Towards safe self-distillation of internet-scale text-to-image diffusion models. In *ICML 2023 Workshop on Challenges in Deployable Generative AI*.
- [24] Sanghyun Kim, Seohyeon Jung, Balhae Kim, Moonseok Choi, Jinwoo Shin, and Juho Lee. 2024. GitHub - nannullna/safe-diffusion: The official implementation of the paper "Towards Safe Self-Distillation of Internet-Scale Text-to-Image Diffusion Models" (ICML 2023 Workshop on Challenges in Deployable Generative AI) — github.com. <https://github.com/nannullna/safe-diffusion>.
- [25] Jennifer Korn. 2023. Getty Images suing the makers of popular AI art tool for allegedly stealing photos. In *CNN Business*. CNN. <https://www.cnn.com/2023/01/17/tech/getty-images-stability-ai-lawsuit/index.html>
- [26] Ziyi Kou, Shichao Pei, Yijun Tian, and Xiangliang Zhang. 2023. Character As Pixels: A Controllable Prompt Adversarial Attacking Framework for Black-Box Text Guided Image Generation Models. In *Proceedings of the Thirty-Second International Joint Conference on Artificial Intelligence, IJCAI-23*, Edith Elkind (Ed.). International Joint Conferences on Artificial Intelligence Organization, 983–990. <https://doi.org/10.24963/ijcai.2023/109> Main Track.
- [27] Nupur Kumari, Bingliang Zhang, Sheng-Yu Wang, Eli Shechtman, Richard Zhang, and Jun-Yan Zhu. 2023. Ablating Concepts in Text-to-Image Diffusion Models.
- [28] Nupur Kumari, Bingliang Zhang, Sheng-Yu Wang, Eli Shechtman, Richard Zhang, and Jun-Yan Zhu. 2023. GitHub - nupurkmr9/concept-ablation: Ablating Concepts in Text-to-Image Diffusion Models (ICCV 2023) — github.com. <https://github.com/nupurkmr9/concept-ablation>.
- [29] Seung Hyun Lee, Wonseok Roh, Wonmin Byeon, Sang Ho Yoon, Chanyoung Kim, Jinkyu Kim, and Sangpil Kim. 2022. Sound-Guided Semantic Image Manipulation. In *Proceedings of the IEEE/CVF Conference on Computer Vision and Pattern Recognition (CVPR)*. 3377–3386.
- [30] Xinfeng Li, Yuchen Yang, Jiangyi Deng, Chen Yan, Yanjiao Chen, Xiaoyu Ji, and Wenyuan Xu. 2024. SafeGen: Mitigating Unsafe Content Generation in Text-to-Image Models. arXiv:2404.06666 [cs.CV]
- [31] Weixin Liang, Yuhui Zhang, Yongchan Kwon, Serena Yeung, and James Zou. 2022. Mind the Gap: Understanding the Modality Gap in Multi-modal Contrastive Representation Learning. In *NeurIPS*. <https://openreview.net/forum?id=S7Evt2t9uit3>
- [32] Tsung-Yi Lin, Michael Maire, Serge J. Belongie, Lubomir D. Bourdev, Ross B. Girshick, James Hays, Pietro Perona, Deva Ramanan, Piotr Dollár, and C. Lawrence Zitnick. 2014. Microsoft COCO: Common Objects in Context. *CoRR* abs/1405.0312 (2014). arXiv:1405.0312 <http://arxiv.org/abs/1405.0312>
- [33] Jiachen Ma, Anda Cao, Zhiqing Xiao, Jie Zhang, Chao Ye, and Junbo Zhao. 2024. Jailbreaking Prompt Attack: A Controllable Adversarial Attack against Diffusion Models. arXiv:2404.02928 [cs.CR]
- [34] Aleksander Madry, Aleksandar Mkelov, Ludwig Schmidt, Dimitris Tsipras, and Adrian Vladu. 2018. Towards Deep Learning Models Resistant to Adversarial Attacks. In *6th International Conference on Learning Representations, ICLR 2018, Vancouver, BC, Canada, April 30 - May 3, 2018, Conference Track Proceedings*. OpenReview.net. <https://openreview.net/forum?id=rjzIBFZAAb>
- [35] Meg Matthias. 2023. Why does AI art screw up hands and fingers? <https://www.britannica.com/topic/Why-does-AI-art-screw-up-hands-and-fingers-2230501>
- [36] Midjourney. 2024. Midjourney. www.midjourney.com. [Accessed 15-04-2024].
- [37] David A. Noever and Samantha E. Miller Noever. 2021. Reading Isn't Believing: Adversarial Attacks On Multi-Modal Neurons. arXiv:2103.10480 [cs.LG]
- [38] Minh Pham, Kelly O. Marshall, Niv Cohen, Govind Mittal, and Chinmay Hegde. 2023. Circumventing Concept Erasure Methods For Text-to-Image Generative Models. arXiv:2308.01508 [cs.LG]

- [39] Minh Pham, Kelly O. Marshall, Chinmay Hegde, and Niv Cohen. 2024. Robust Concept Erasure Using Task Vectors. arXiv:2404.03631 [cs.CV]
- [40] Stable Diffusion Negative Prompt. [n.d.]. Negative prompt. <https://github.com/AUTOMATIC1111/stable-diffusion-webui/wiki/Negative-prompt>.
- [41] Yiting Qu, Xinyue Shen, Xinlei He, Michael Backes, Savvas Zannettou, and Yang Zhang. 2023. GitHub - YitingQu/unsafe-diffusion - github.com. <https://github.com/YitingQu/unsafe-diffusion/tree/main>.
- [42] Yiting Qu, Xinyue Shen, Xinlei He, Michael Backes, Savvas Zannettou, and Yang Zhang. 2023. Unsafe Diffusion: On the Generation of Unsafe Images and Hateful Memes From Text-To-Image Models. In *ACM SIGSAC Conference on Computer and Communications Security (CCS)*. ACM.
- [43] Alec Radford, Jong Wook Kim, Chris Hallacy, Aditya Ramesh, Gabriel Goh, Sandhini Agarwal, Girish Sastry, Amanda Askell, Pamela Mishkin, Jack Clark, Gretchen Krueger, and Ilya Sutskever. 2021. Learning Transferable Visual Models From Natural Language Supervision. In *Proceedings of the 38th International Conference on Machine Learning, ICML 2021, 18-24 July 2021, Virtual Event (Proceedings of Machine Learning Research, Vol. 139)*, Marina Meila and Tong Zhang (Eds.), PMLR, 8748–8763. <http://proceedings.mlr.press/v139/radford21a.html>
- [44] Aditya Ramesh, Rishabh Goyal, Alessandro Sordani, Yaniv Ovadia, and Geoffrey E. Hinton. 2021. DALL-E 2: The Flower That Blooms in Adversity. In *OpenAI Blog*. <https://openai.com/blog/dall-e-2/>
- [45] Javier Rando, Daniel Paleka, David Lindner, Lennart Heim, and Florian Tramèr. 2022. Red-Teaming the Stable Diffusion Safety Filter. arXiv:2210.04610 [cs.AI]
- [46] Robin Rombach, Andreas Blattmann, Dominik Lorenz, Patrick Esser, and Björn Ommer. 2022. High-Resolution Image Synthesis With Latent Diffusion Models. In *Proceedings of the IEEE/CVF Conference on Computer Vision and Pattern Recognition (CVPR)*, 10684–10695.
- [47] Robin Rombach, Andreas Blattmann, Dominik Lorenz, Patrick Esser, and Björn Ommer. 2022. High-Resolution Image Synthesis With Latent Diffusion Models. In *Proceedings of the IEEE/CVF Conference on Computer Vision and Pattern Recognition (CVPR)*, 10684–10695.
- [48] Robin Rombach, Andreas Blattmann, Dominik Lorenz, Patrick Esser, and Björn Ommer. 2023. stabilityai/stable-diffusion-2-1 · Hugging Face — huggingface.co. <https://huggingface.co/stabilityai/stable-diffusion-2-1>.
- [49] Patrick Schramowski, Manuel Brack, Björn Deiseroth, and Kristian Kersting. 2023. Safe Latent Diffusion: Mitigating Inappropriate Degeneration in Diffusion Models. In *Proceedings of the IEEE Conference on Computer Vision and Pattern Recognition (CVPR)*.
- [50] Christoph Schuhmann, Romain Beaumont, Richard Vencu, Cade W Gordon, Ross Wightman, Theo Coombes, Aarush Katta, Clayton Mullis, Mitchell Wortsman, Patrick Schramowski, Srivatsa R Kundurthy, Katherine Crowson, Ludwig Schmidt, Robert Kaczmarczyk, and Jenia Jitsev. 2022. Laion-5b: An open large-scale dataset for training next generation image-text models. In *Thirty-sixth Conference on Neural Information Processing Systems Datasets and Benchmarks Track*. 1–2.
- [51] Haz Sameen Shahgir, Xianghao Kong, Greg Ver Steeg, and Yue Dong. 2024. Asymmetric Bias in Text-to-Image Generation with Adversarial Attacks. arXiv:2312.14440 [cs.LG]
- [52] G. Somepalli, V. Singla, M. Goldblum, J. Geiping, and T. Goldstein. 2023. Diffusion Art or Digital Forgery? Investigating Data Replication in Diffusion Models. In *2023 IEEE/CVF Conference on Computer Vision and Pattern Recognition (CVPR)*. IEEE Computer Society, Los Alamitos, CA, USA, 6048–6058. <https://doi.org/10.1109/CVPR52729.2023.00586>
- [53] Yu-Lin Tsai, Chia-Yi Hsu, Chulin Xie, Chih-Hsun Lin, Jia-You Chen, Bo Li, Pin-Yu Chen, Chia-Mu Yu, and Chun-Ying Huang. 2024. Ring-A-Bell! How Reliable are Concept Removal Methods For Diffusion Models?. In *The Twelfth International Conference on Learning Representations*. <https://openreview.net/forum?id=lm7MRcsFiS>
- [54] Aäron van den Oord, Yazhe Li, and Oriol Vinyals. 2018. Representation Learning with Contrastive Predictive Coding. arXiv:1807.03748 <http://arxiv.org/abs/1807.03748>
- [55] JULES VERNE. 2024. *Twenty Thousand Leagues under the sea*. ALADDIN BOOKS.
- [56] Xueyang Wang and Xiaozhang Liu. 2021. Enhancing Robustness of Classifiers Based on PCA. In *2021 4th International Conference on Pattern Recognition and Artificial Intelligence (PRAI)*. 336–341. <https://doi.org/10.1109/PRAI53619.2021.9550807>
- [57] Yuxin Wen, Neel Jain, John Kirchenbauer, Micah Goldblum, Jonas Geiping, and Tom Goldstein. 2023. Hard Prompts Made Easy: Gradient-Based Discrete Optimization for Prompt Tuning and Discovery. In *Thirty-seventh Conference on Neural Information Processing Systems*. <https://openreview.net/forum?id=VOstHxDdsN>
- [58] Jing Wu, Trung Le, Munawar Hayat, and Mehrtash Harandi. 2024. EraseDiff: Erasing Data Influence in Diffusion Models. arXiv:2401.05779 [cs.CV]
- [59] Yutong Wu, Jie Zhang, Florian Kerschbaum, and Tianwei Zhang. 2023. Backdooring Textual Inversion for Concept Censorship. arXiv:2308.10718 [cs.CR]
- [60] Chaowei Xiao, Zhongzhu Chen, Kun Jin, Jiong Xiao Wang, Weili Nie, Mingyan Liu, Anima Anandkumar, Bo Li, and Dawn Song. 2022. Densepure: Understanding diffusion models towards adversarial robustness. In *arXiv preprint arXiv:2211.00322*.
- [61] Wenhan Yang, Jingdong Gao, and Baharan Mirzasoleiman. 2023. Robust Contrastive Language-Image Pretraining against Data Poisoning and Backdoor Attacks. In *Thirty-seventh Conference on Neural Information Processing Systems*. <https://openreview.net/forum?id=ONwL9ucoYG>
- [62] Yijun Yang, Ruiyuan Gao, Xiao Yang, Jianyuan Zhong, and Qiang Xu. 2024. GuardT2I: Defending Text-to-Image Models from Adversarial Prompts. arXiv:2403.01446 [cs.CV]
- [63] Yuchen Yang, Bo Hui, Haolin Yuan, Neil Gong, and Yinzhi Cao. 2024. Sneaky Prompt: Jailbreaking Text-to-image Generative Models. In *Proceedings of the IEEE Symposium on Security and Privacy*.
- [64] Eric Zhang, Kai Wang, Xingqian Xu, Zhangyang Wang, and Humphrey Shi. 2023. Forget-Me-Not: Learning to Forget in Text-to-Image Diffusion Models. In *arXiv preprint arXiv:2211.08332*.
- [65] Eric Zhang, Kai Wang, Xingqian Xu, Zhangyang Wang, and Humphrey Shi. 2023. GitHub - SHI-Labs/Forget-Me-Not: Forget-Me-Not: Learning to Forget in Text-to-Image Diffusion Models, 2023 — github.com. <https://github.com/SHI-Labs/Forget-Me-Not>.
- [66] Jiawei Zhang, Zhongzhu Chen, Huan Zhang, Chaowei Xiao, and Bo Li. 2023. {DiffSmooth}: Certifiably robust learning via diffusion models and local smoothing. In *32nd USENIX Security Symposium (USENIX Security 23)*. 4787–4804.

APPENDIX

A RETENTION OF ADVERSARIAL NOISE

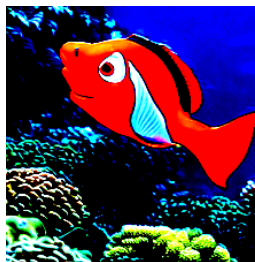
WARNING: This work includes an inappropriate image which has been redacted. Reader discretion is advised.



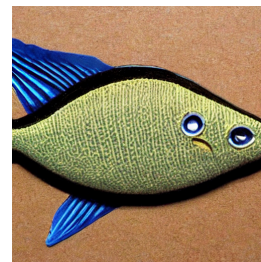
(a) Adversarial Image of Nudity



(b) Generated Approximation of Adversarial Image for Nudity



(c) Adversarial Image of Nemo



(d) Generated Approximation of Adversarial Image for Nemo



(e) Adversarial Image of Elon Musk



(f) Generated Approximation for Adversarial Image for Elon Musk

Figure 4: (Left) x^{adv} generated by PGD against ESPRESSO; (right) Images generated from adversarial prompts of x^{adv}